Supporting Information

Dehydrogenation of Ammonia-Borane Employing an Air-stable, Phosphine-free Molecular Nickel Pincer Catalyst

Bijan Mondal,[†a] Aisa Mohanty,[†a] Prosenjit Daw[a*]

[a] Department of Chemical Sciences, Indian Institute of Science Education and Research Berhampur, Transit Campus, (Govt. ITI Building), Engg. School Junction, Berhampur 760010, Odisha, India

Corresponding Author: Email id: pdaw@iiserbpr.ac.in

Contents

1. General Experimental Details

All experiments were carried out either inside a nitrogen-filled glovebox or using standard Schlenk techniques, unless specified otherwise. All chemicals were obtained from commercial suppliers and, unless noted, used as received without further purification. $NaBD_4$ (98 atom% D) was purchased from Sigma-Aldrich. $NiCl_2 \cdot 6H_2O$ was obtained from Loba Chemie, and $NiCl_2(PPh_3)_2$ was prepared according to a reported literature procedure.[1] Ammonia Borane (AB) was prepared following the literature procedure.[2] Deuterated ammonia borane (NH_3BD_3, ND_3BH_3, ND_3BD_3) was prepared and characterised following the literature procedure.[3] For the catalysis reaction setup, the sealed Schlenk Tube, with Plain Sidearm (25 mL volume) was used. All the solvents were pre-dried according to the literature procedures. THF, n-hexane, 1,4-dioxane and diethyl ether were dried by distillation in the presence of benzophenone and sodium metal. Dichloromethane and toluene were distilled from calcium hydride and stored under a 4 Å molecular sieve. Methanol and ethanol were dried by distillation from magnesium turnings and iodine cake. ^1H and ^{13}C NMR spectra were recorded on a 400 MHz Bruker AVANCE NEO Ascend spectrometer. Chemical shifts (δ) are reported in parts per million (ppm) and referenced to the residual proton signal of the deuterated solvent: $CDCl_3$ (δ 7.26 ppm), DMSO-d_6 (δ 2.50 ppm), H_2O in DMSO-d_6 (δ 3.33 ppm), C_6D_6 (δ 7.16 ppm), and H_2O (δ 4.79 ppm). Coupling constants (J) are given in hertz (Hz). Paramagnetic ^1H NMR spectra were collected over a range of 0–90 ppm with a spectral width of 250 ppm. Proton-decoupled $^{13}C\{^1H\}$ NMR spectra were referenced to the central carbon signal of $CDCl_3$ (δ 77.15 ppm). Proton-coupled ^{11}B NMR spectra were referenced to $BF_3 \cdot Et_2O$ (δ 0.00 ppm). NMR signal multiplicities are abbreviated as follows: s = singlet, d = doublet, t = triplet, q = quartet, dd = doublet of doublets, m = multiplet. Mass spectra were recorded on an Xevo G2-XS QT of a Quadrupole Time of Flight Mass spectrometer, Waters. The evolved hydrogen gas was analysed on TRACE 1610 gas chromatography (TCD, CARBOXENTM 1000 column, Ar carrier gas flow, Thermo Scientific). IR spectra were recorded on a Bruker TENSOR II FT-IR Spectrometer. UV-Vis were recorded by using a JASCO V-770 spectrometer. Elemental analysis was done using the UNICUBE CHNSO element analyser. On an XtaLAB Synergy-R diffractometer, the single-crystal data were collected. The diffractometer utilises a DW system (monochromated Cu Kα (λ = 1.54184) or Mo Kα (λ = 0.71073)) radiation and features a HyPix detector. The data were gathered at low temperatures. The intensity data were processed using the Rigaku suite of data processing tools (data collection: CrysAlis PRO system (CCD 43.116a 64-bit), cell refinement and data reduction: CrysAlis PRO 1.171.43116a (Rigaku OD, 2024)).

SHELXS (Sheldrick, 2008) was used to refine the structure, and CrysAlisPro 1.171.43.116a was used to apply absorption corrections (Rigaku Oxford diffraction, 2024). 2,2':6',2''-terpyridine (**L3**) and 6,6''-dibromo-2,2':6',2''-terpyridine were prepared using a literature procedure.[4,5]

Safety Note. Extreme caution should be used when carrying out the AB dehydrogenation reactions, as the release of hydrogen can lead to sudden pressurisation of reaction vessels.

2. Ligand synthesis

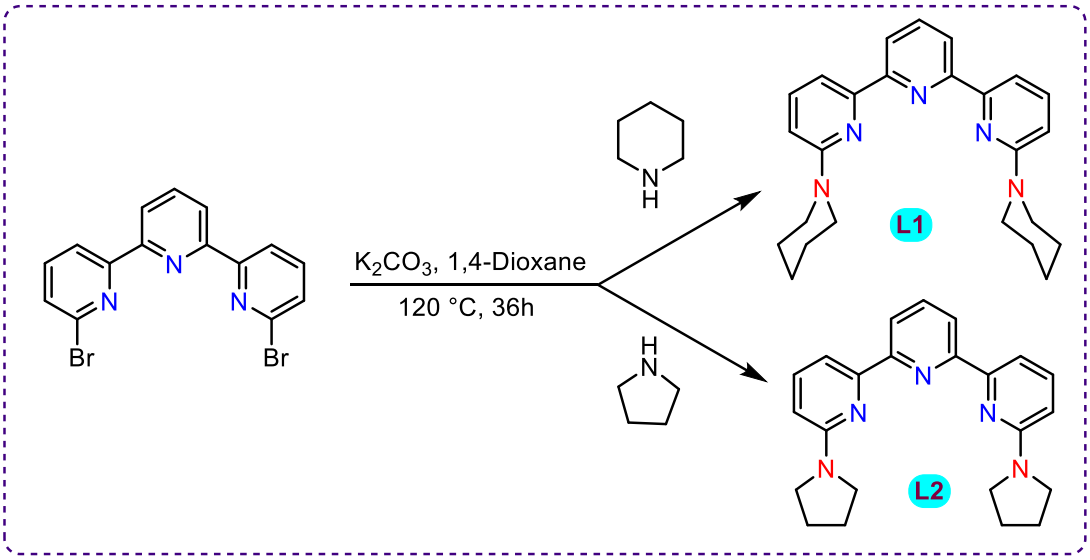

Scheme S1. Reaction scheme of ligands (**L1** and **L2**) synthesis.

2.1. Synthesis of ligand L1:

Ligand **L1** was prepared according to the literature procedure.[6]

2.2. Synthesis of 6,6''-di(pyrrolidin-1-yl)-2,2':6',2''-terpyridine (L2):

In a nitrogen-filled sealed tube, 6,6''-dibromo-2,2':6',2''-terpyridine (0.511mmol, 1 equiv.), pyrrolidine (3.58 mmol, 7 equiv.), K_2CO_3 (3.58 mmol,7 equiv.), and 1,4-dioxane (5 mL) were combined and degassed by flushing with N_2. The reaction mixture was stirred at 120 °C for 36 h. Upon completion, the solvent was removed under reduced pressure, and the residue was diluted with distilled water (15 mL). The aqueous phase was subsequently extracted with dichloromethane (3 × 20 mL). The combined organic layer was washed with a brine solution, dried over Na_2SO_4, and evaporated to dryness to obtain a light-yellow solid product (**L2**) (0.323 mmol, 63%).

^{1}H NMR (400 MHz, $CDCl_3$) δ (ppm) 8.41 (d, J = 7.8 Hz, 2H), 7.91 (d, J = 7.4 Hz, 2H), 7.85 (t, J = 7.8 Hz, 1H), 7.60 (t, J = 7.9 Hz, 2H), 6.41 (d, J = 8.4 Hz, 2H), 3.57 (t, J = 6.7 Hz, 8H), 2.04 (t, J = 3.3 Hz, 8H).

^{13}C NMR (101 MHz, $CDCl_3$) δ (ppm)= 156.94, 156.02, 154.49, 137.64, 137.07, 120.19, 108.59, 106.56, 77.21, 77.01, 76.69, 46.67, 25.58.

HRMS (m/z) = 372.2196 ([**L2**+H]$^{+}$, **L2** = $C_{23}H_{25}N_5$

Elemental analysis for [$C_{23}H_{25}N_5$.0.5 CH_2Cl_2] Analy calc: C: 68.19; H: 6.33; N: 16.92, Found: C: 69.08; H: 6.587; N: 16.49.

IR (ATR) υ (cm^{-1}) = 2920, 2851, 2116,1715,1593, 1492, 1419, 1265, 1160, 777, 741, 664, 662, 625, 561.

3. Metal complexes synthesis

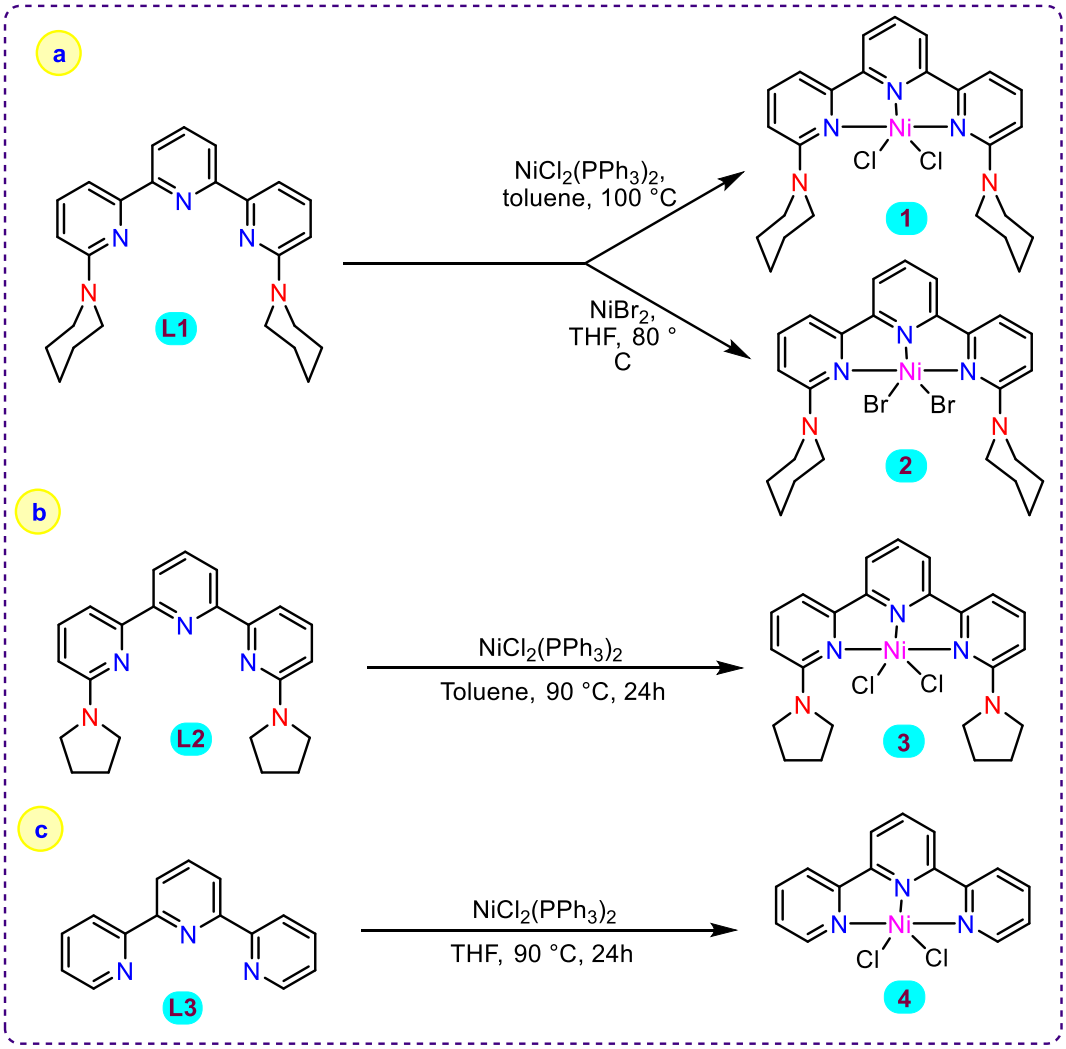

Scheme S2: Reaction scheme of metal complexes (**1-4)** synthesis.

3.1. Synthesis of complexes 1 and 2:

Complexes **1** and **2** have been prepared according to the literature procedure.[7] The single crystal X-ray analysis of complex **2** was obtained by growing suitable crystals from the slow diffusion of diethyl ether vapour into a dichloromethane-methanol solution at -15 °C. The molecular crystal structure of complex **2** was described in Section 9.1.

3.2. Synthesis of complex 3:

In a 25 mL Schlenk tube, ligand **L2** (0.107 mmol, 1 equiv.) and metal precursor $[NiCl_2(PPh_3)_2]$ (0.107 mmol, 1 equiv.) were added with 10 mL of dry toluene. The reaction mixture was kept at 90 °C for 24 h, and a greenish-yellow colour solution appeared. After 24 hours, the yellow residue was filtered off from the solution, washed with dry diethyl ether (3 × 10 mL), and dried under reduced pressure to afford a yellow solid as complex **3** (0.0887 mmol, 83%). A paramagnetic ^1H NMR was recorded in $CDCl_3$ in a 0-90 ppm range; SW = 250 ppm.

HRMS (m/z) = 464.1165 ([**3**-Cl]$^+$, **3**= $C_{23}H_{25}Cl_2N_5Ni$).

Elemental analysis for $[C_{23}H_{25}Cl_2N_5Ni.0.5CH_2Cl_2]$ Analy. calc: C: 51.93; H: 4.82; N: 12.88; Found: C; 52.07; H; 4.80; N; 12.49.

IR (ATR) υ (cm^{-1}) = 3360, 3078, 2958, 2875, 1973, 1611, 1558, 1487, 1442, 1346, 1100, 1005, 927, 813, 785, 639, 580.

The single crystal X-ray analysis of complex **3** was obtained by growing suitable crystals from the slow diffusion of diethyl ether vapour into a dichloromethane-methanol solution at -15 °C. The molecular crystal structure of complex **3** was described in Section 9.2.

3.3. Synthesis of complex 4:

In a 25 mL Schlenk tube, ligand **L3** (0.128 mmol, 1 equiv.) and $NiCl_2(PPh_3)_2$ (0.128 mmol, 1 equiv) were dissolved in 10 mL of dry THF. The reaction mixture was kept at 90 °C for 24 h, during which a sea-green-coloured solution formed. After the reaction was completed, the THF was removed under reduced pressure, and the resulting solid was washed with diethyl ether (3 × 10 mL) and dried under vacuum to afford a sea-green solid (0.110 mmol, 85%).

HRMS (m/z) = 325.9846 ([**4**-Cl]$^+$, **4** = $C_{15}H_{11}Cl_2N_3Ni$)
Elemental analysis for $[C_{15}H_{11}Cl_2N_3Ni.MeOH]$ Analy calc: C: 48.66; H: 3.83; N: 10.64 found: C: 47.71; H: 3.69; N:10.52.

IR (ATR) υ (cm^{-1}) = 3356, 3061, 1597, 1574, 1487, 1406, 1316, 1299, 1182, 1097, 980, 837, 775, 737, 667, 542, 517.

The single crystal X-ray analysis of complex **4** was obtained by growing suitable crystals from the slow diffusion of diethyl ether vapour into a dichloromethane-methanol solution at -15 °C. The molecular crystal structure of complex **4** was described in Section 9.3.

4. General procedure for catalytic ammonia borane dehydrogenation

All the catalytic reactions were set up in the nitrogen-filled glove box. AB (1 mmol), Ni catalysts (in mol%) and degassed dry THF solvent (1 mL) were added to a sidearm sealed tube. The tube was taken out of the glove box and placed in a preheated oil bath at a specified temperature. Upon addition of the catalyst to the ammonia borane solution at room temperature, the reaction mixture changed in colour from bright yellow to muddy green. Upon heating, this mixture gradually darkened and eventually formed a brown slurry. The evolved gas volume was measured by an inverted water burette method. For gas chromatography analysis, a gas sample was taken from the reaction tube. Borazine is volatile and sensitive to air and moisture; therefore, after gas measurement, the tube was transferred to the glove box, where $NaBPh_4$ (0.01 mmol) was added as an internal standard for ^{11}B NMR analysis (Table S1).

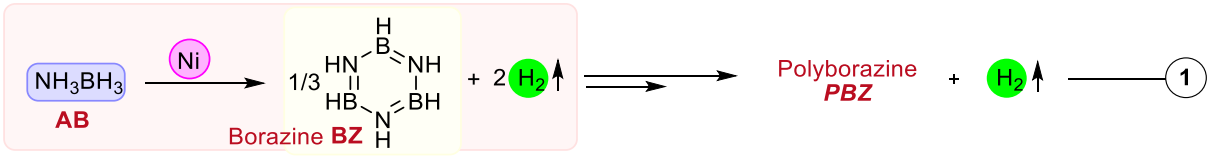

The formation of H_2 gas (in mmol) and the % yield of BZ was calculated using equation 1.

- mmol of hydrogen gas produced = vol. of hydrogen gas produced (mL) / 22.46 (mol/L)
- The equivalent of hydrogen produced = mmol of hydrogen produced / mmol of AB initially fed
- Turnover number (TON) = mmol of hydrogen gas produced/ mmol of catalyst loading
- Turn over frequency (TOF) = TON/t (t in h)
- mmol of borazine produced = {(mmol of internal standard / 3) * $\int B3N3H6$ }
- % yield of Borazine: [{(mmol of internal standard / 3) * $\int B3N3H6$ }/ theoretical yield of BZ] x 100

4.1. Optimisation of Catalytic dehydrogenation of AB in the presence of Ni catalysts

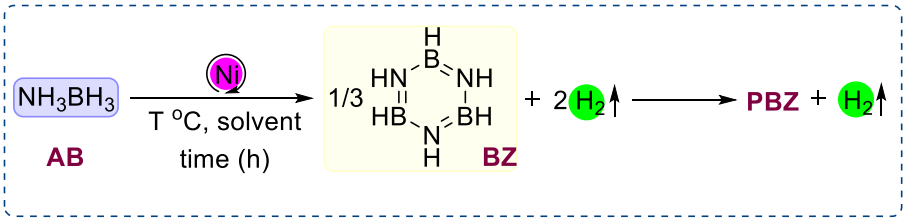

Table S1: Optimisation table for Catalytic dehydrogenation of AB in the presence of Ni catalysts.

Entry	Ni Cat	Solvent	Temp (°C)	Time (h)	H_2 volume in mL (equiv.)	Yield of BZ (%)
1	**1**	THF	60	12	42 (1.86)	29
2[a)]	**1**	THF	60	12	24 (1.07)	20
3	**1**	THF	25	12	4 (0.18)	nd
4	**1**	THF	60	6	26 (1.16)	13
5	**-**	THF	60	12	28 (1.24)	10
6[b)]	**1**	THF	60	12	40 (1.78)	26
7	**1**	Dioxane	60	12	41 (1.83)	23
8	**1**	DME	60	12	14 (0.63)	10
9	**$NiCl_2(PPh_3)_2$**	THF	60	12	22 (0.98)	6
10	**$NiCl_2$**	THF	60	12	33 (1.46)	20
11	**2**	THF	60	12	42 (1.86)	28
12	**3**	THF	60	12	36 (1.60)	20
13	**1**	THF	60	48	48 (2.14)	58
14	**1**	THF	80	12	54 (2.40)	61
15	**1**	THF	80	48	58 (2.58)	52
16[c)]	**1**	THF	60	12	28 (1.24)	6
17	**1**	Toluene	60	12	9 (0.40)	nd
18	**1**	Diethyl ether	60	12	7 (0.31)	nd
19[d)]	**1**	THF	60	12	6 (0.26)	nd
20[e)]	**1**	THF	60	12	2 (0.08)	nd

Reaction condition: AB (1 mmol), Ni Cat (1 mol%), solvent (1 mL); yield of Borazine was determined by ^{11}B NMR with $NaBPh_4$ (0.01 mmol) as an internal standard. a)

complex **1** was taken in 0.5 mol%. b) Hg (100 equiv. w.r.t **1**) was added. c) PPh_3 added 5 equiv. w.r.t to complex **1**. d) $Me_2NH.BH_3$ (1 mmol). e) $Me_3N.BH_3$ (1 mmol).

4.2. AB dehydrogenation GC-TCD analysis of gas purity

In a N_2-filled glovebox, a 25 mL sidearm-sealed tube was charged sequentially with catalyst **1** (1 mol%), AB (1 mmol), in 1 mL of THF. The tube was placed in a preheated oil bath at 60 °C for 12 h. After completion of the reaction, the tube was cooled to room temperature, and the gas phase was analysed by gas chromatography using argon as the carrier gas. Hydrogen gas was detected with a retention time of 0.82 min (Figure S1).[8]

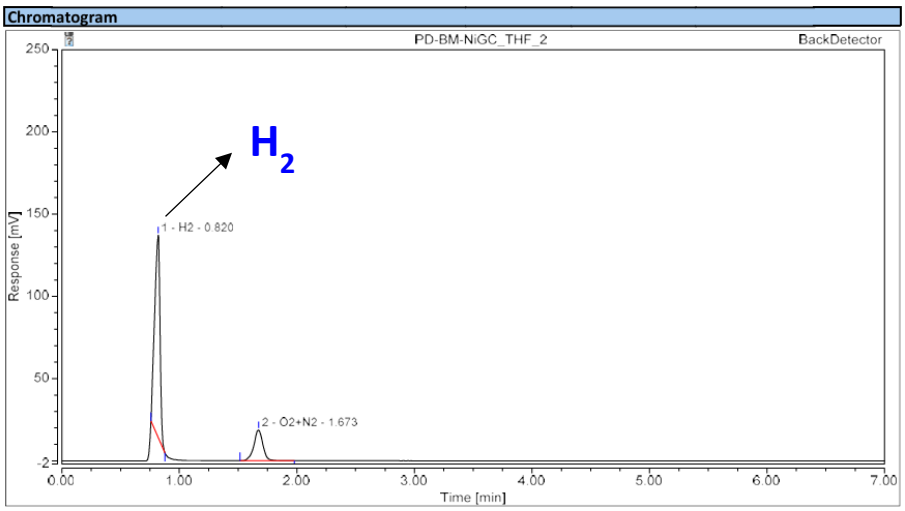

Figure S1. GC-TCD analysis of hydrogen gas evolved from the catalytic dehydrogenation of AB (Table S1, entry 1). A small peak at 1.673 min was observed for the residual N_2 and O_2 mixture.

5. Control Experiments

5.1. Catalyst durability test for the AB dehydrogenation

In a 25 mL sidearm sealed tube, **1** (1 mol%) and AB (1 mmol) were added in 1 mL of THF in a N_2-filled glove box. The reaction tube was placed in a preheated oil bath at 80 °C for 12 hours. After completion of the reaction, the tube was cooled to room temperature and the H_2 gas was measured through the inverted water burette method. Following the 1st cycle, the sequential cycles were performed by adding 1 mmol AB, with 0.4 mL of THF in each cycle, to the same reaction mixture. The H_2 gas was collected in each cycle. The process was repeated up to the 9th cycle (Figure S2).

Complex **1** loading = 1 mol%

Total gas volume (in mL) = 414 mL

Overall catalytic TON = 1843

No. of cycles	1	2	3	4	5	6	7	8	9
H_2 gas vol. (in mL)	54	52	52	52	50	54	52	48	42

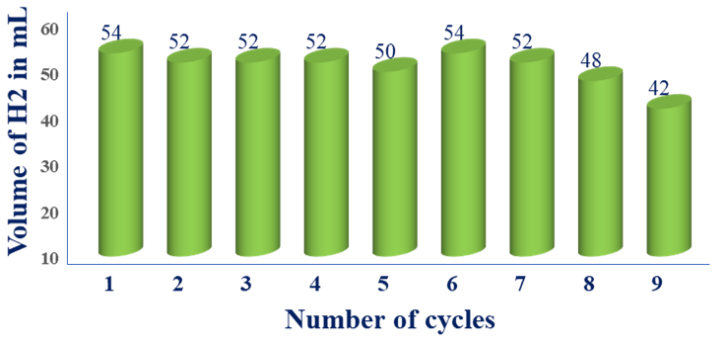

Figure S2. Bar diagram of the evolved H_2 gas in mL with the number of catalytic cycles.

5.2. Monitoring the progress of the reaction by measuring the gas volume evolved

In a 25 mL sidearm sealed tube, **1** (0.01 mmol) and AB (3 mmol) were added in 1 mL of THF in a N_2-filled glove box. The reaction tube was then removed from the glove box and placed in a preheated oil bath at 80 °C to initiate the reaction. The progress of gas evolution was monitored over time up to 31 h, with the tube cooled to room temperature before each measurement. The initial TOF was determined from the reaction progress during the first 1 h (Figure S3).

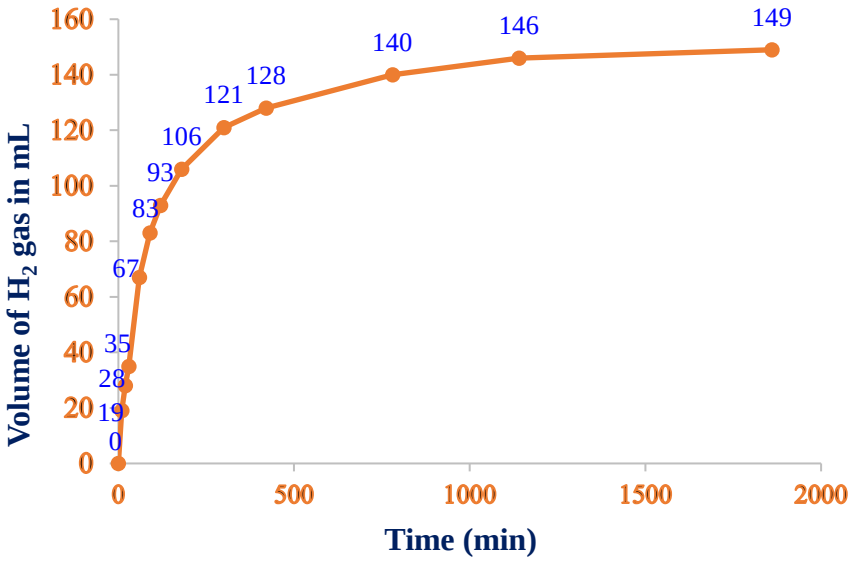

Figure S3. The time course profiles of the catalytic dehydrogenation of AB.

Initial TOF (in h^{-1}) = mmol of hydrogen gas produced / mmol of catalyst feed × t (in h)

= (2.98 mmol of H_2 gas / 0.01 mmol of catalyst loading) × 1 h

= 298 h^{-1}

5.3. Chemical entrapment technique during dehydrogenation of AB

Inside the glove box, AB (0.1 mmol, 1 equiv.) and complex **1** (0.001 mmol, 0.01 equiv.) were taken in an NMR tube with 0.5 ml of dry THF. The NMR tube was removed from the glove box and analysed by ^{11}B NMR at room temperature. Again, the NMR tube was taken to the glovebox, and to this cyclohexene (2 mmol, 20 equiv.) was added. Afterwards, ^{11}B NMR analysis was performed from room temperature to 60 °C over a time duration of 12 h to 24 h. It was observed that, at 12 h, 60 °C, a peak at -4.95 ppm resulted, which might be due to the formation of $H_2NBH(C_6H_{11})$ along with a peak at +47.8 ppm, confirming the formation of $H_2NB(C_6H_{11})_2$ observed in the ^{11}B NMR spectrum.[9] However, after 24 h, 60 °C, only the formation of $H_2NB(C_6H_{11})_2$ was detected, indicating the complete entrapment of cyclohexene under the catalytic reaction conditions (Figure S4). When a similar reaction was performed without the catalyst, the reaction proceeded with slow consumption of AB, where at 24 h, 60 °C, only the intermediate $H_2NBH(C_6H_{11})$ resulted (Figure S5).

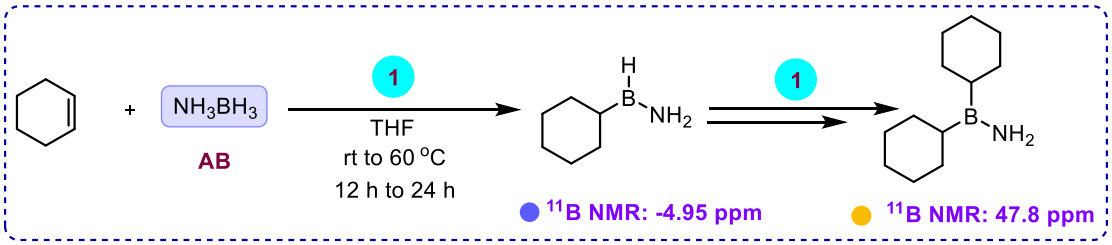

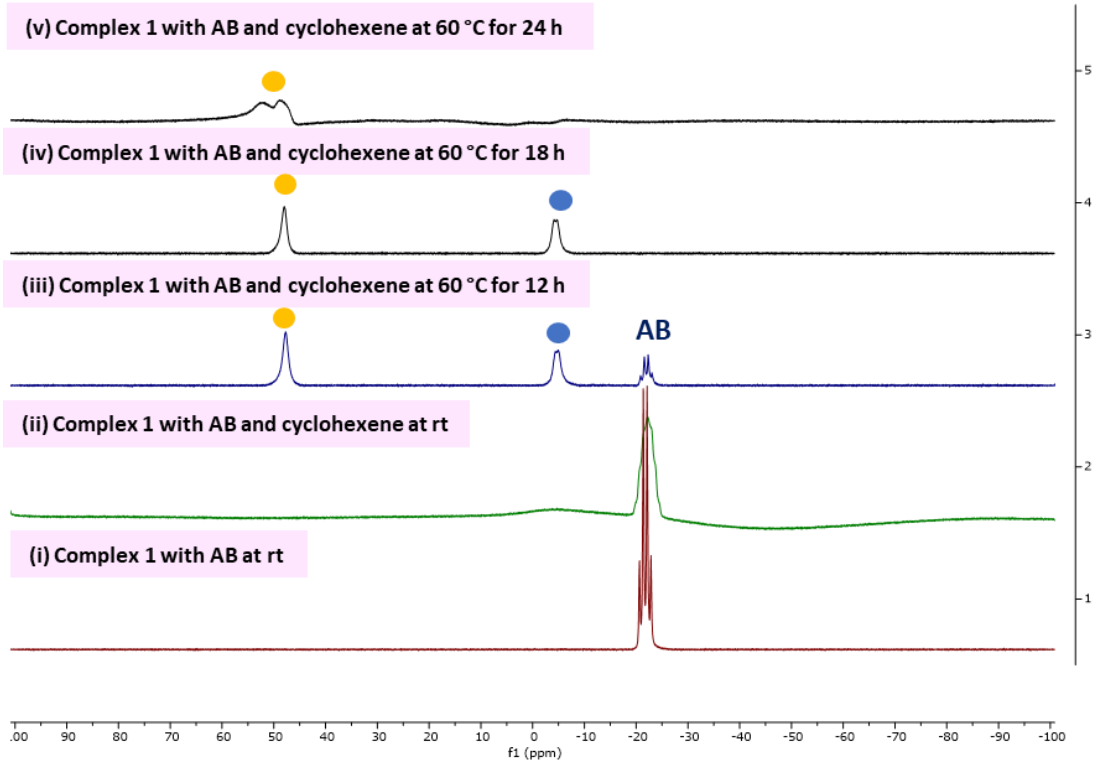

Figure S4. ^{11}B NMR analysis of chemical entrapment of cyclohexene with AB in the presence of complex **1**.

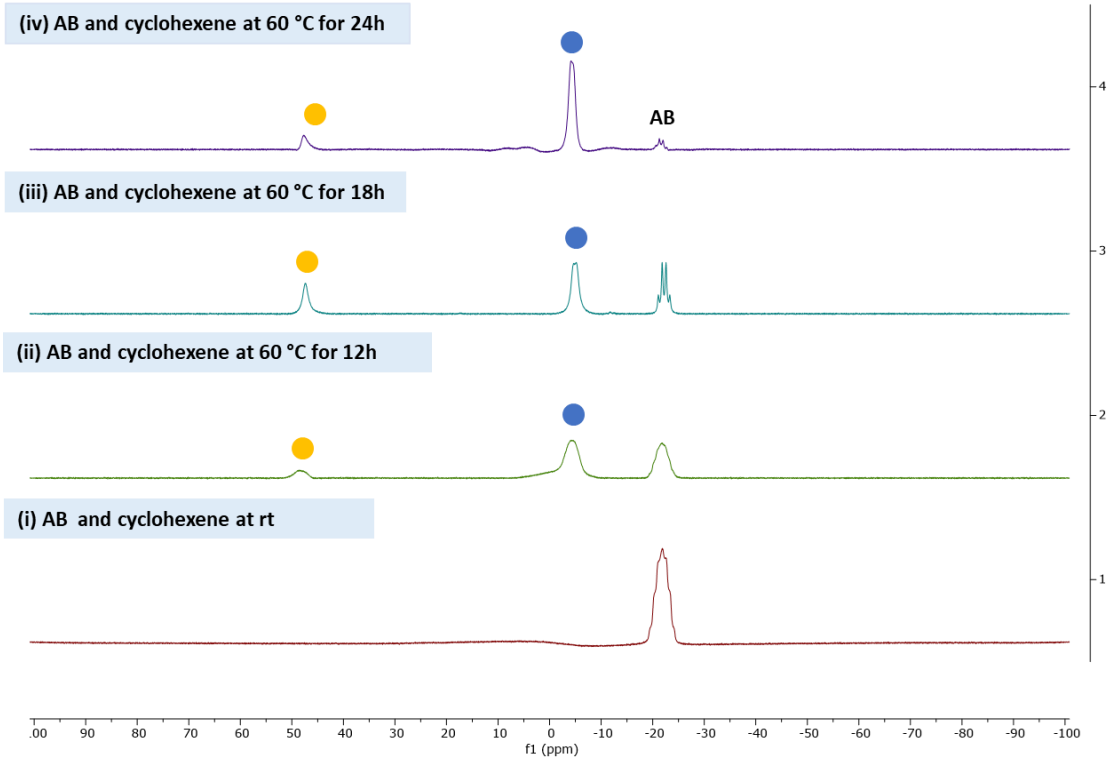

Figure S5. ^{11}B NMR analysis of chemical entrapment of cyclohexene with AB in the absence of complex **1**.

5.4. Detection of the resulting boron intermediates in BZ formation

Inside the nitrogen-filled glove box, AB (0.1 mmol, 1 equiv.) and complex **1** (0.01 mmol, 0.1 equiv.) were placed in an NMR tube with 0.5 mL of a THF/C_6D_6 (1:1) solvent mixture. The NMR tube was then removed from the glove box and analysed by ^{11}B NMR at room temperature and at 80 °C from 15 min to 8 h. It was observed that at room temperature, a short-lived intermediate NH_3BH_2Cl was observed at δ = -8.60 ppm along with unreacted AB. When the mixture was heated to 80 °C for 15 minutes to 4 h, the NH_3BH_2Cl signal disappeared, and new peaks appeared: a triplet at δ = -11.33 ppm corresponding to B-(cyclotriborazanyl)amine-borane (BCTB), a peak at δ = -26.2 ppm corresponding to μ-amidodiborane (μ-AMD), and a peak at δ = 31.03 ppm corresponding to BZ. After heating for up to 8 h at 80 °C, AB, μ-AMD, and BCTB were mostly consumed, leaving BZ as the main product (Figure S6). Similarly, ND_3BH_3 and NH_3BD_3 were utilised as the substrate instead of AB. The monitored ^{11}B NMR depicted the slow consumption of the substrate to generate the deuterated BZ ($[D]_n$-BZ) (Figures S7-S8).

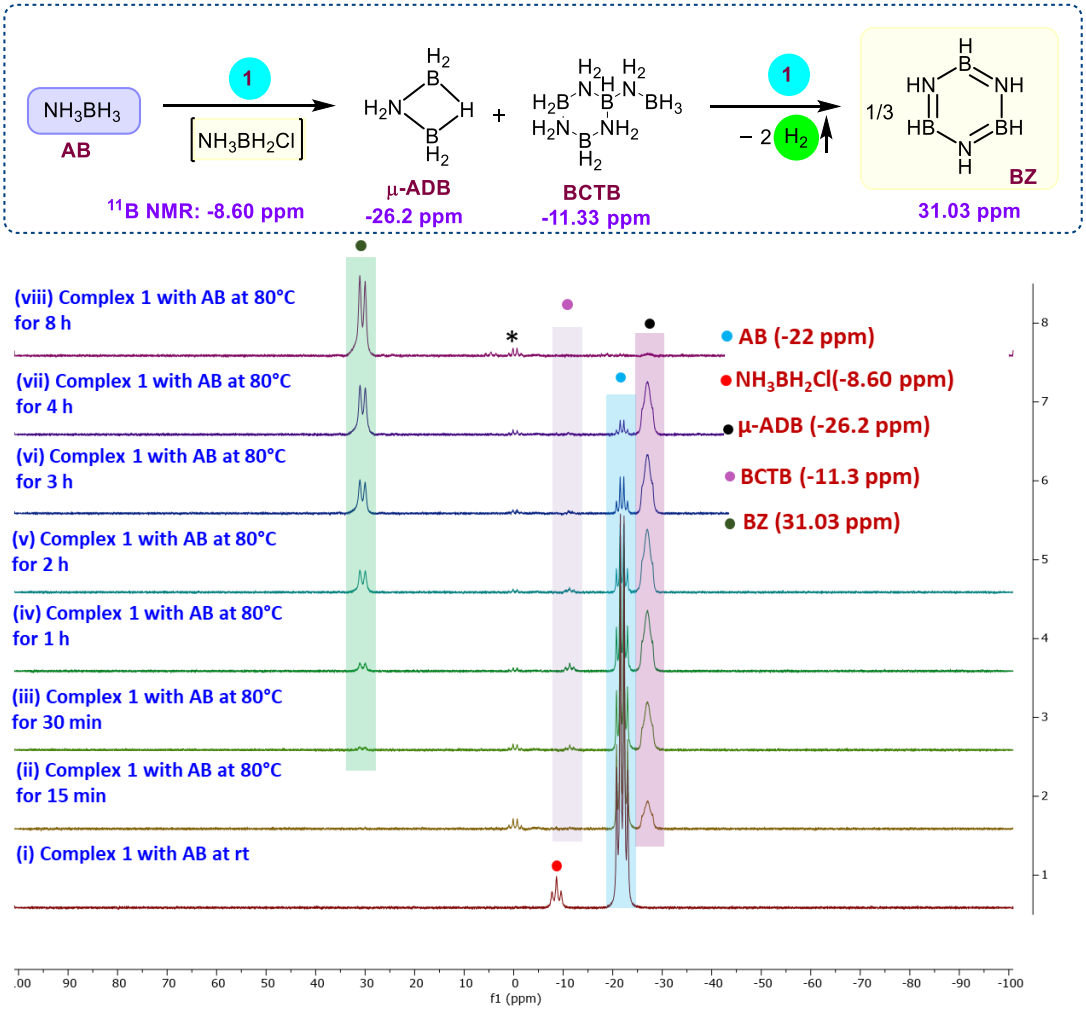

Figure S6. ^{11}B NMR analysis spectra monitoring the progress catalytic transformation of AB to BZ using complex 1; * = Unidentified species

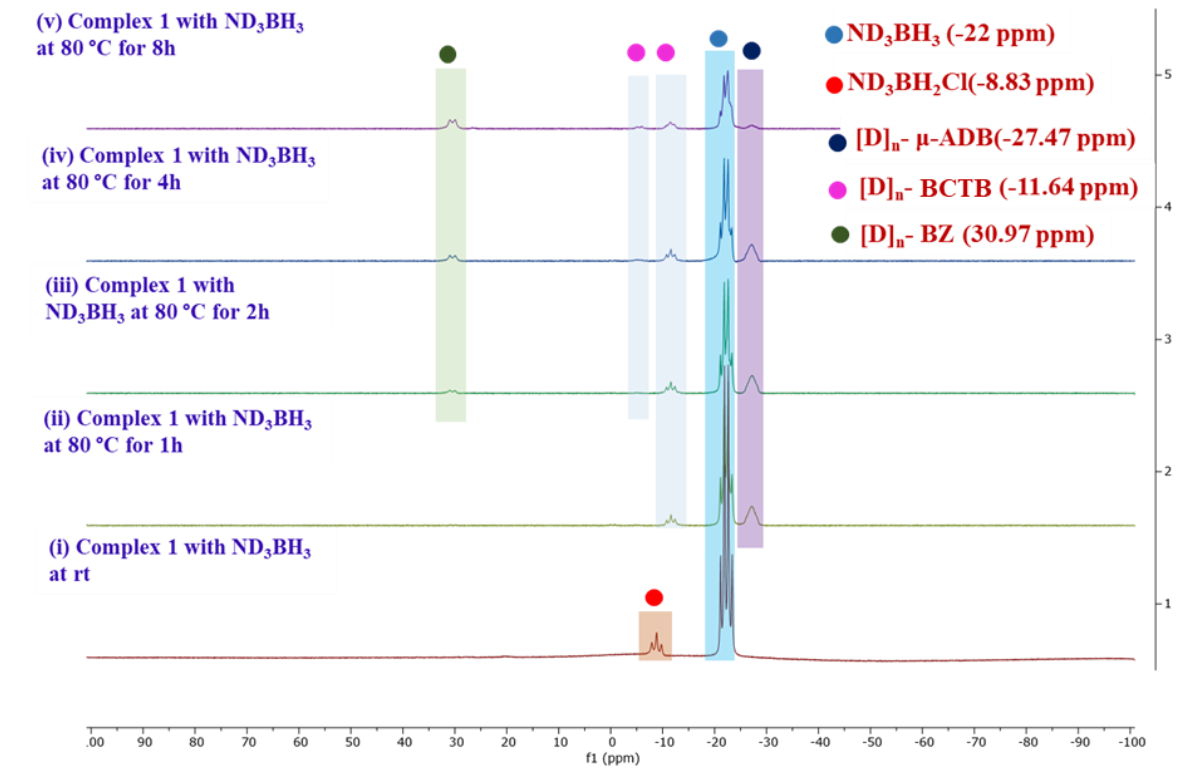

Figure S7. ^{11}B NMR analysis spectra monitoring the progress catalytic transformation of ND_3BH_3 to deuterated BZ using complex **1.**

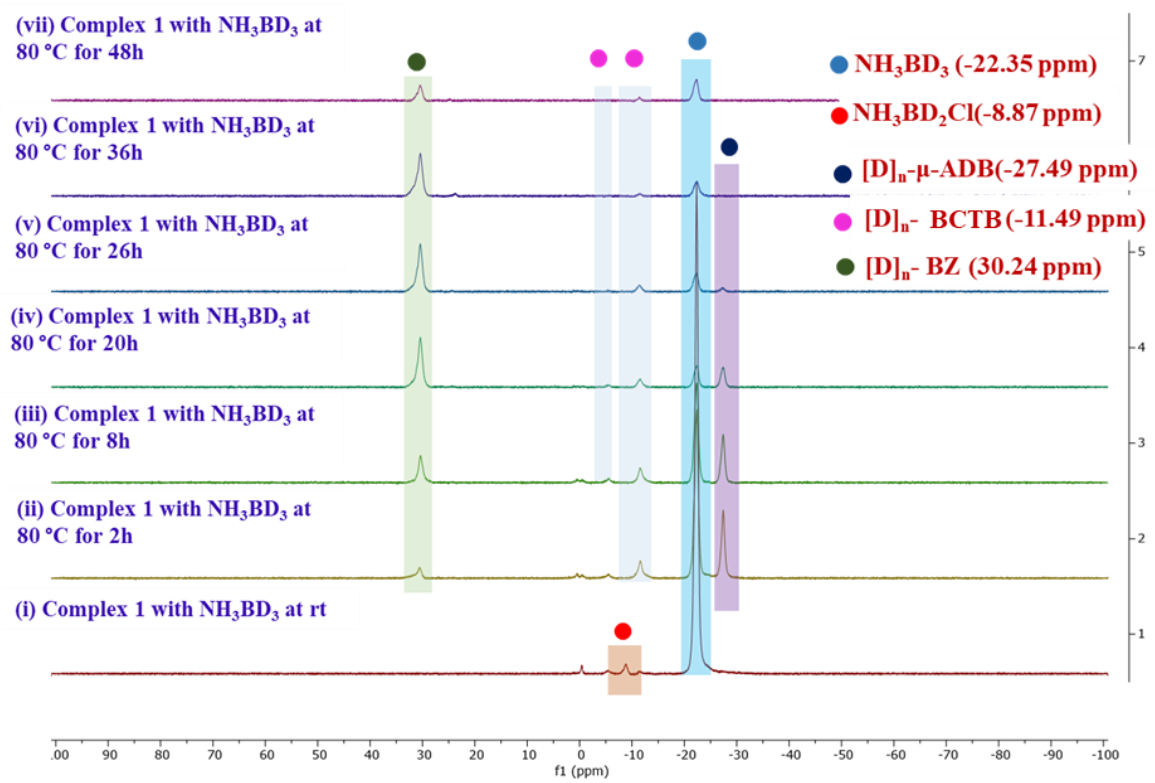

Figure S8. ^{11}B NMR analysis spectra monitoring the progress catalytic transformation of NH_3BD_3 to deuterated BZ using complex **1.**

5.5. IR spectroscopy of B-N coupled product

Once the catalytic dehydrogenation of AB was completed, after analyzing the gas evolution and the ^{11}B NMR spectra, the H_2-depleted material produced in the AB dehydrogenation reactions was taken for measurement by IR spectroscopy. IR spectrum was taken from after the reaction at **(a)**1 mmol AB, 1 mol% complex **1**, 60 °C, 12 h, 1 ml THF (Table S1, entry 1) and **(b)** 1 mmol AB, 1 mol% complex **1**, 80 °C, 12 h, 1 ml THF (Table S1, entry 14) and The IR spectrum was found to be consistent with the remaining mixture of polyborazine/ polyborazylene/ poly(aminoborane). In condition **(a),** NH and BH stretching frequencies were observed in the range of 3100-3450 cm^{-1} and 2050-2550 cm^{-1}, respectively. Additionally, bending vibrational modes of NH and BH are observed at 1300-1700 cm^{-1} and 930-1300 cm^{-1}. These spectral features are attributed to a mixture comprising unreacted AB and various boron-coupled products, including polyborazine (soluble in THF), polyborazylene (insoluble in THF) and a small amount of PAB (insoluble in THF). In condition **(b),** where the intensity of B-H and N-H stretching decreases, and B-N stretching appears at 1400 cm^{-1} for the cyclic structure increases, while B-N bending mode was observed at 901 cm^{-1}. (Figure S9).[10,11]

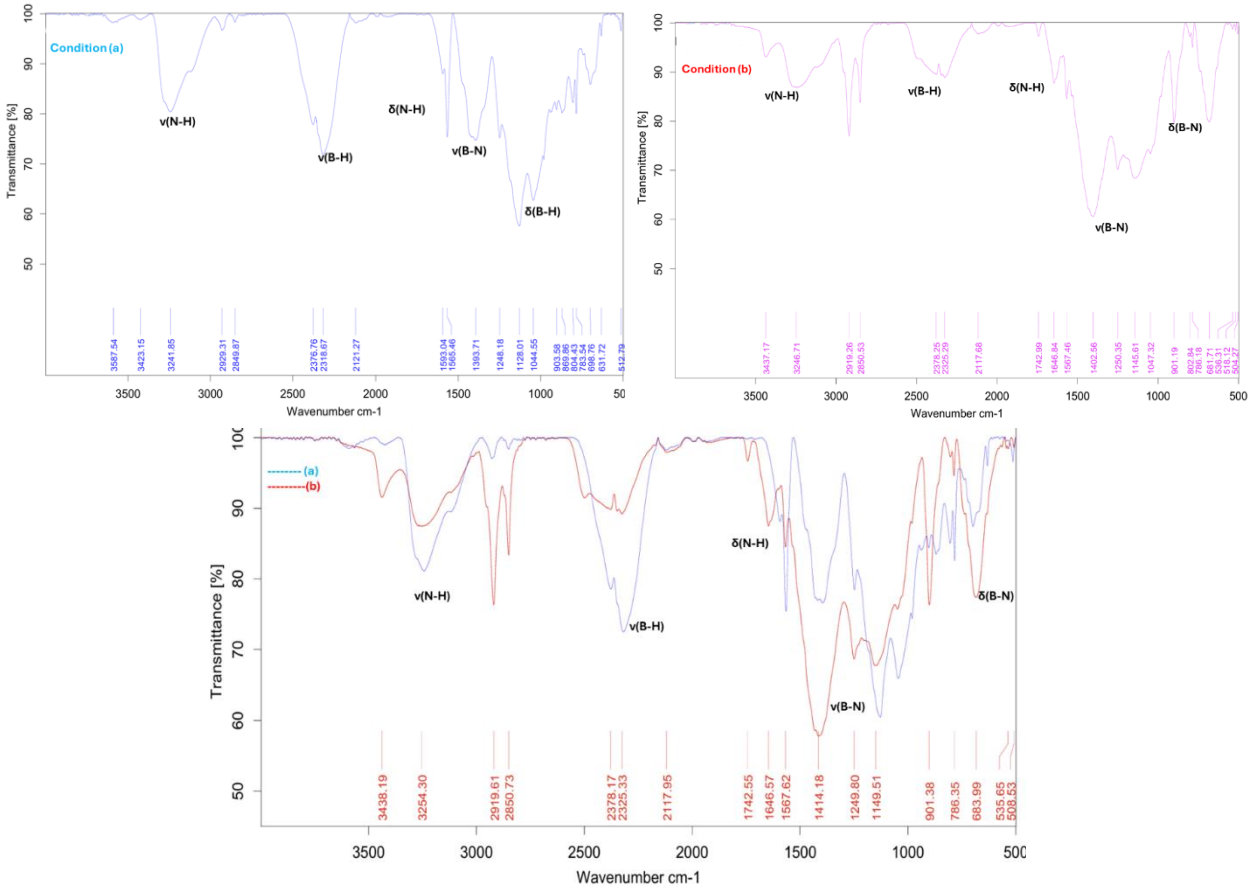

Figure S9. FTIR spectrum of the crude catalytic reaction mixture containing H_2-depleted material produced in the AB dehydrogenation reactions.

5.6. Detection of catalytic TON for the AB dehydrogenation process

In an N_2-filled glovebox, a sealed sidearm tube (25 mL for entries 1 and 2; 100 mL for entries 3 and 4) was charged sequentially with AB (x mmol), complex **1** (y mol%), and THF. The reaction mixture was then placed in a preheated oil bath at 80 °C for 12 h (entries 1 and 2) and 72 h (entries 3 and 4). Upon completion, the reaction tube was cooled to room temperature, and the evolved H_2 gas was quantified using the inverted water burette method. Subsequently, the reaction tube was transferred to the glovebox, where $NaBPh_4$ was introduced as an internal standard for BZ quantification in ^{11}B NMR analysis (Figures S44-S47).

Table S2.

Entry	AB (x mmol)	1 (y mol%)	Time (in h)	H_2 volume in mL	TON	Yield of BZ (%)
1[a)]	1	0.5	12	42	373	31
2[a)]	1	0.1	12	40	1780	29
3[b)]	5	0.01	72	262	23330	53
4[c)]	10	0.005	72	458	40783	51
a) $NaBPh_4$ was taken in 0.01 mmol; b) $NaBPh_4$ was taken in 0.05 mmol; c) $NaBPh_4$ was taken in 0.1 mmol.						

6. Catalytic reactivity with complex 4

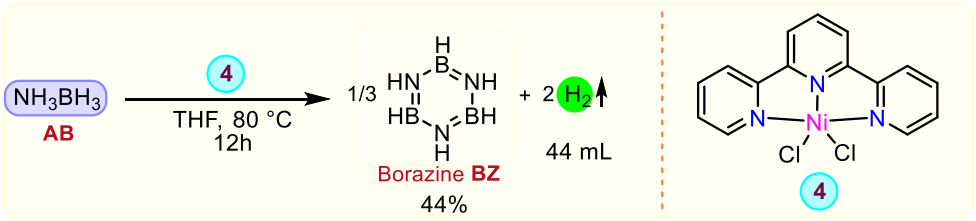

The reaction was conducted according to the general procedure for the catalytic dehydrogenation of AB, as described in Section 4. In a 25 mL sidearm sealed tube, **4** (1 mol%) AB (1 mmol) was added in 1 mL of THF in a N_2-filled glove box. The reaction tube was placed in a preheated oil bath at 80 °C for 12 hours. After the reaction was completed, the tube was cooled to room temperature, and 44 mL of H_2 gas was collected using the inverted water burette method. 44% of BZ was attributed to the ^{11}B NMR analysis using $NaBPh_4$ (0.01 mmol) as an internal standard (Figure S10).

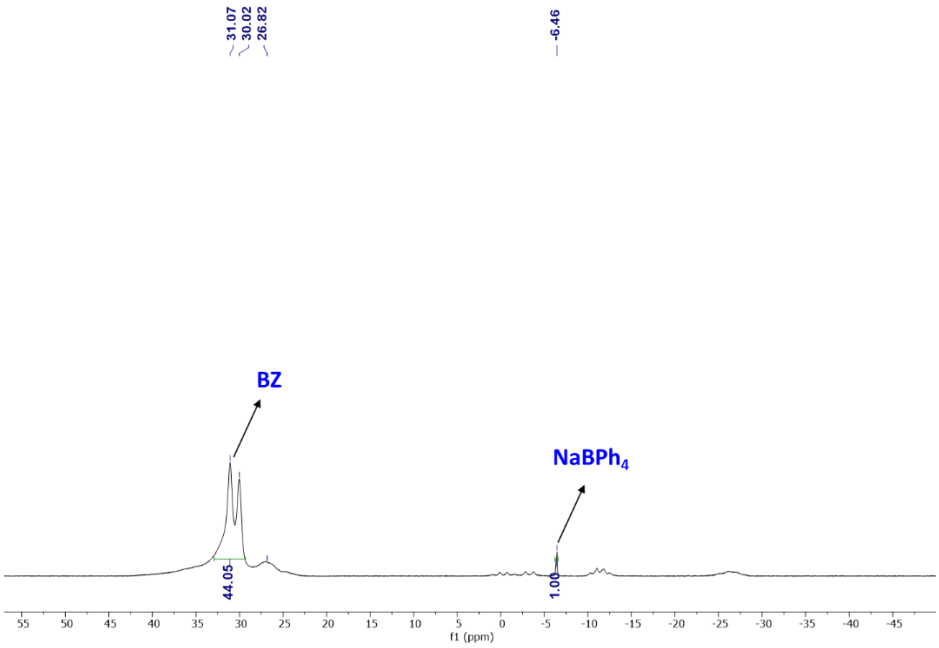

Figure S10. ^{11}B NMR analysis of the crude reaction mixture of AB dehydrogenation utilising complex **4**.

7. Utilization of evolved H_2 gas from the dehydrogenation of AB for styrene hydrogenation catalyzed by Pd/C

In an N_2-filled glovebox, a sealed sidearm tube (reaction tube 1), complex **1** (1 mol%), AB (1 mmol), and THF (1 mL) were added sequentially. Reaction tube **A** was then placed in a preheated oil bath at 80 °C for 12 hours. Upon completion, another sealed sidearm tube (reaction tube **B**) was charged with a solution of styrene (2.5 mmol) in toluene (5 mL), followed by the addition of Pd/C (10 mol%). The air in reaction tube **B** was evacuated through three successive freeze–pump–thaw cycles, and the tube was then maintained under vacuum. Reaction tube **A** was brought to room temperature and subsequently connected to reaction tube **B** through a small silicone tube. Reaction tube **A** was then opened to release the evolved hydrogen gas from AB dehydrogenation process into reaction tube **B**. The reaction mixture in tube **B** was stirred for 24 h, and the yield of ethylbenzene (with respect to the initial styrene feed) was determined by ^{1}H NMR analysis using mesitylene (1 mmol) as an internal standard in $CDCl_3$. $\%Conv._{Styrene}$ = 67%; $\%Yield_{\ Ethyl\ benzene}$ = 66.5% (Figure S11).

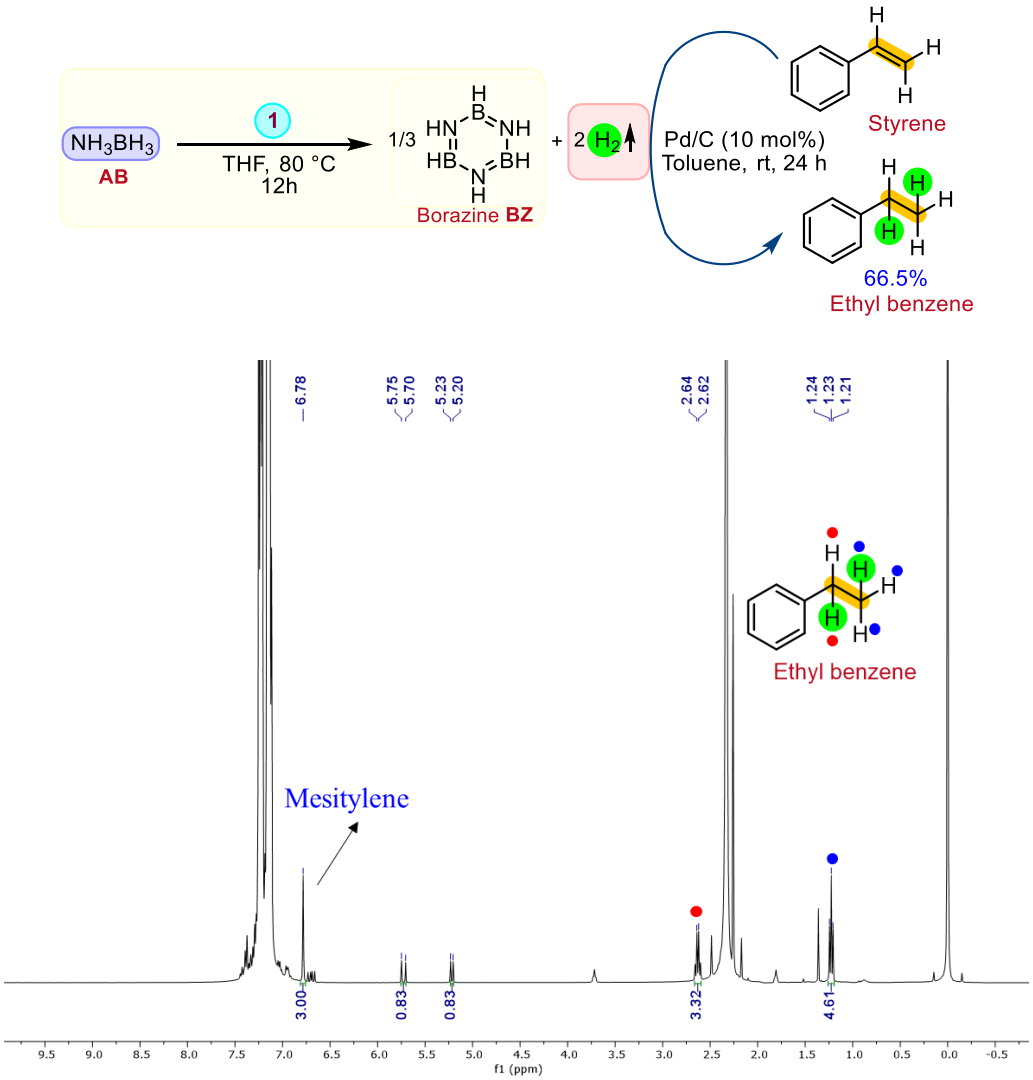

Figure S11. ^{1}H NMR spectrum in $CDCl_3$ of tube **B** reaction mixture Pd/C hydrogenation of styrene using evolved hydrogen produced during AB dehydrogenation process catalyzed by **1**.

8. Spectroscopic data

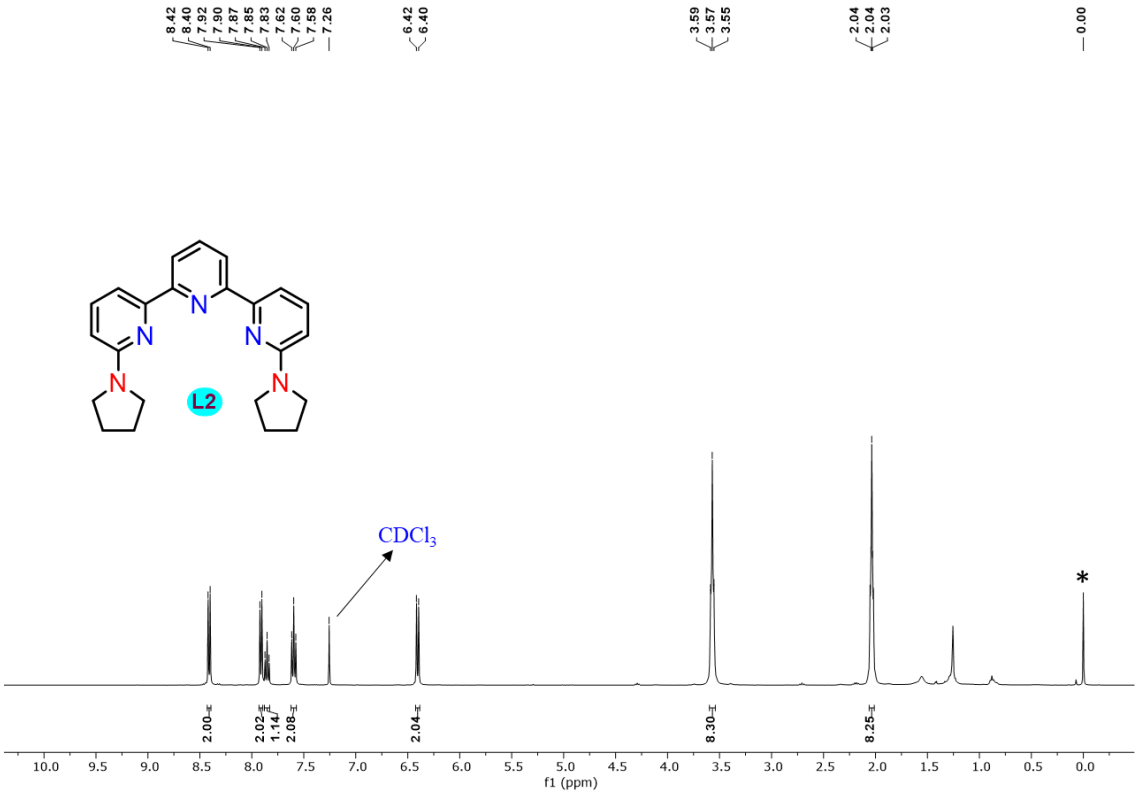

Figure S12. ^{1}H NMR of ligand **L2** in $CDCl_3$. (* = TMS).

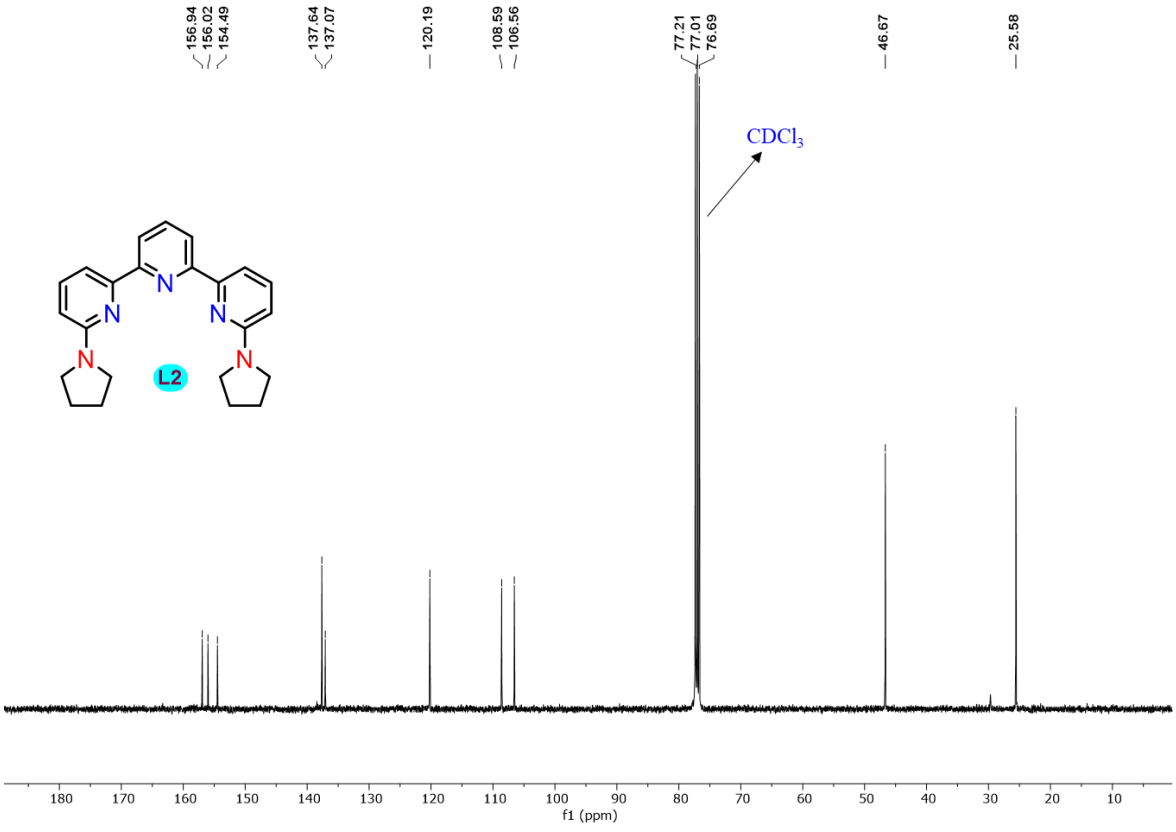

Figure S13. ^{13}C NMR of ligand **L2** in $CDCl_3$.

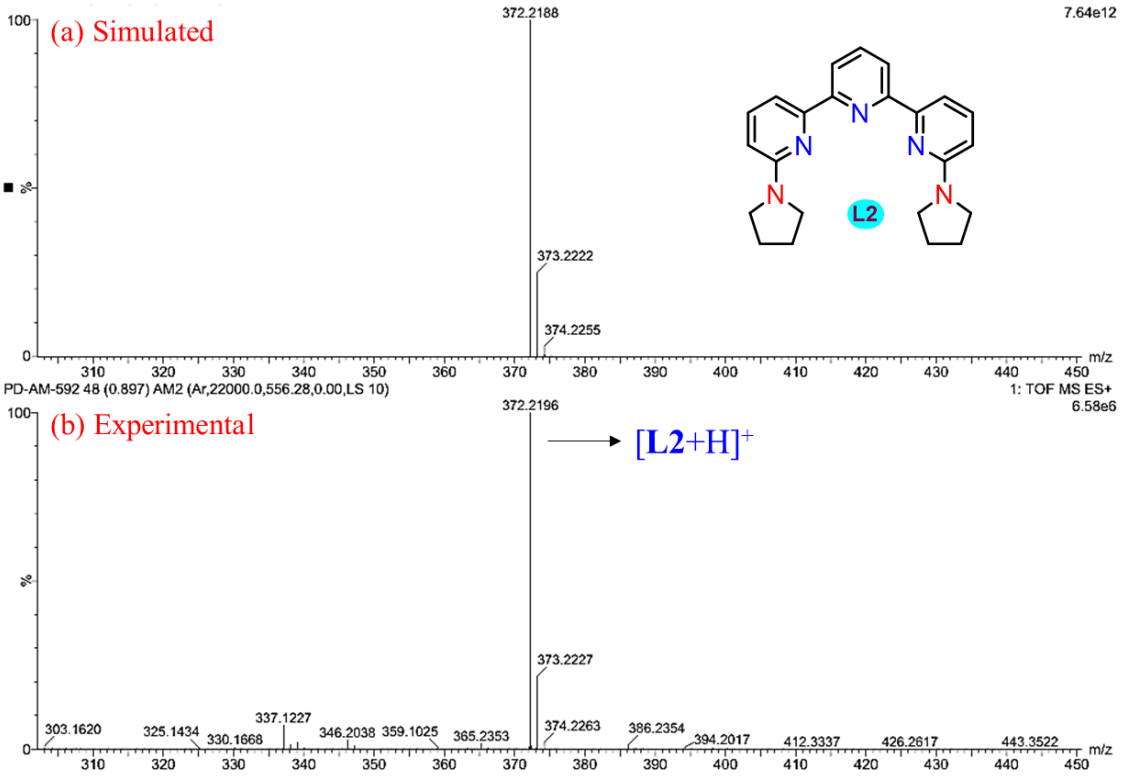

Figure S14. Isotopic mass distribution analysis of ligand **L2**. Simulated (a) and Experimental. (b).

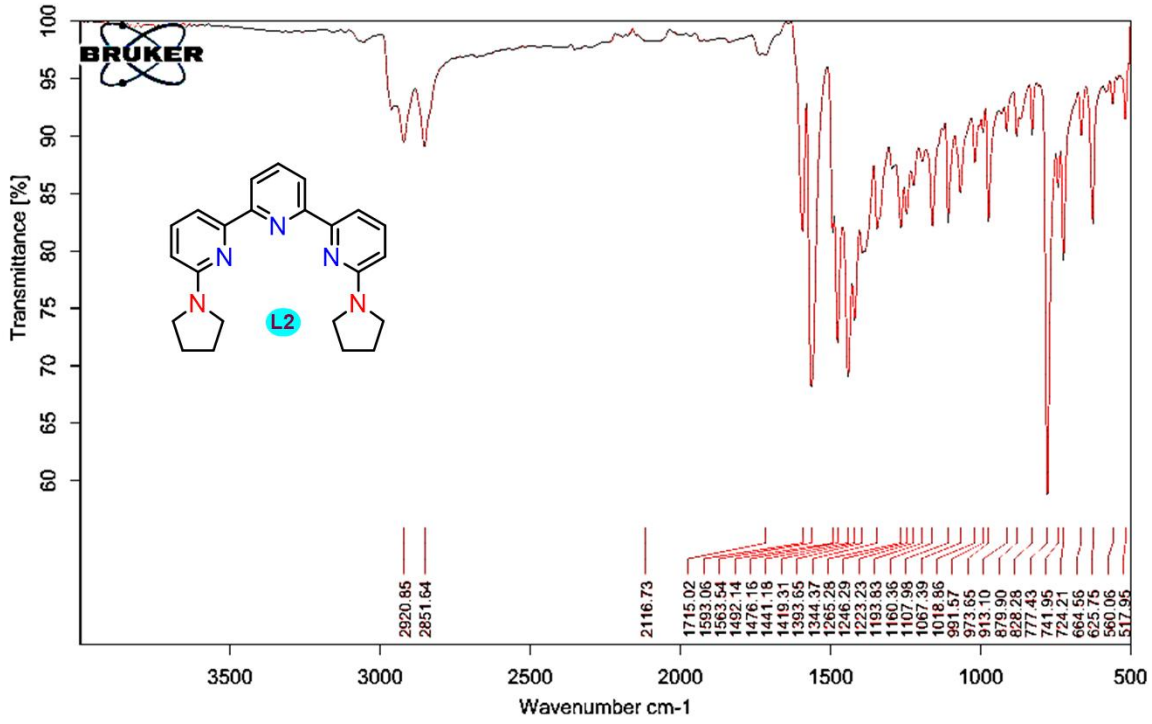

Figure S15. FTIR Spectrum of ligand **L2**.

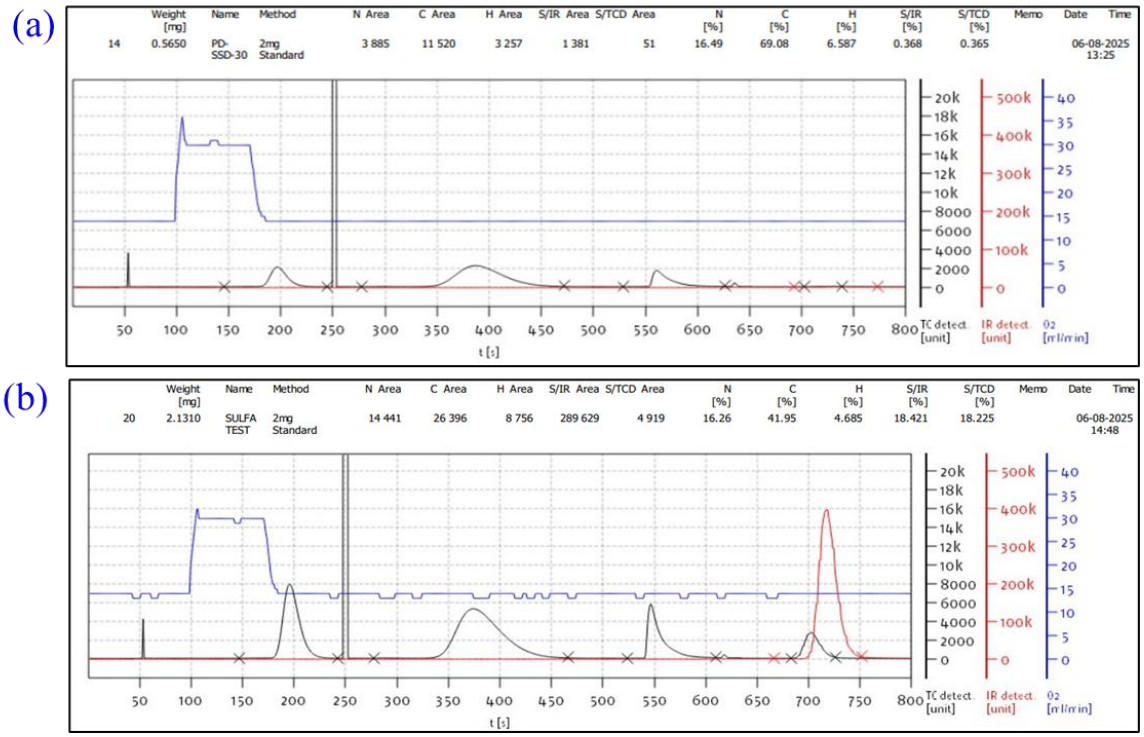

Figure S16. CHNS analysis of ligand **L2** (a) and Sulphanilamide standard test (b).

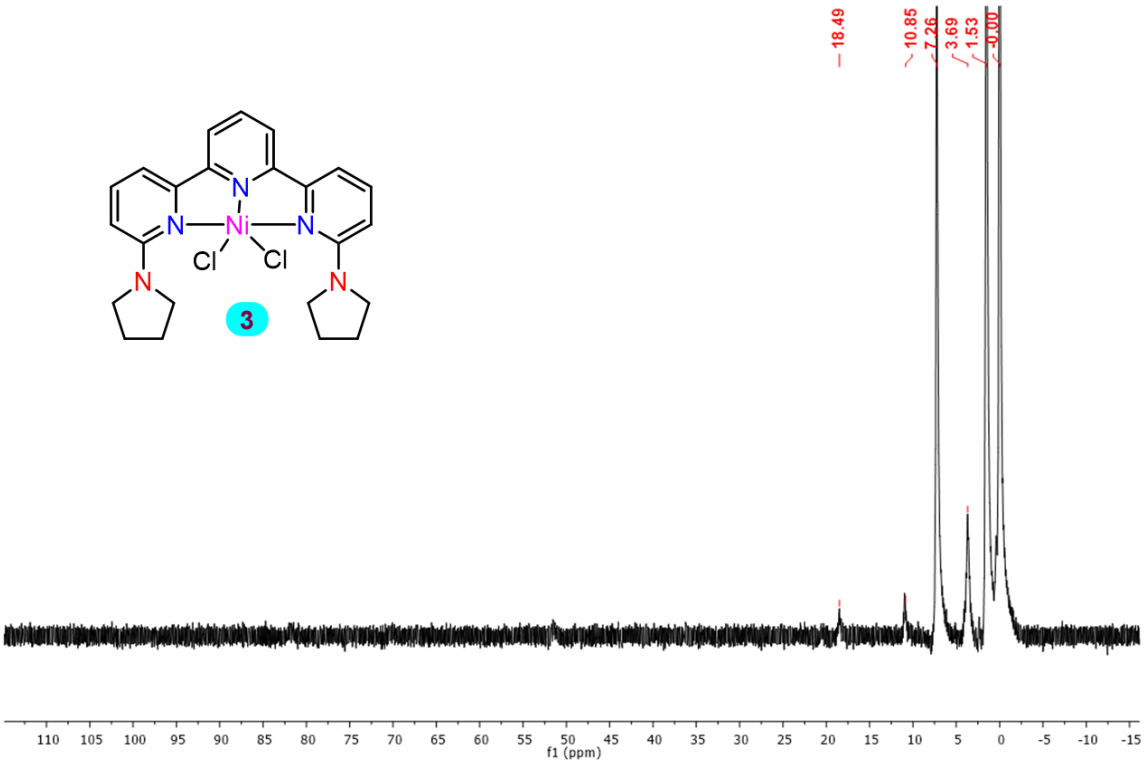

Figure S17. ^{1}H NMR of complex **3** in $CDCl_3$.

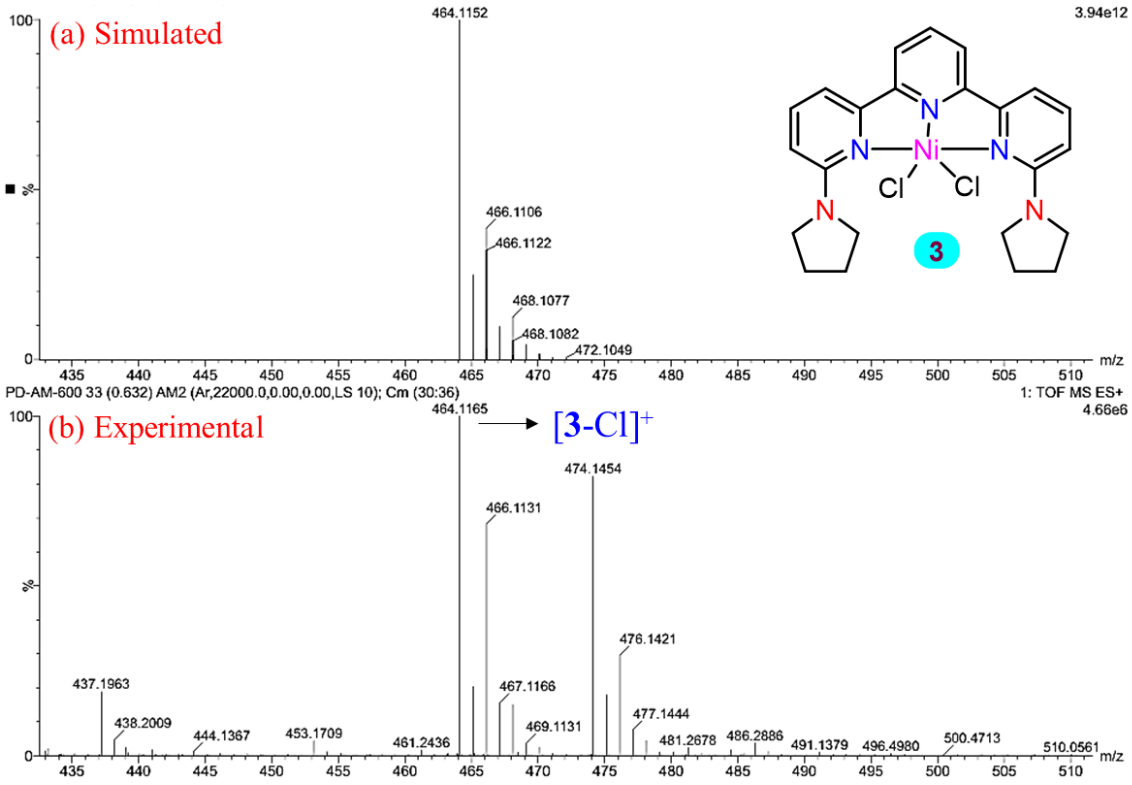

Figure S18. Isotopic mass distribution analysis of complex **3**. Simulated (a) and Experimental. (b).

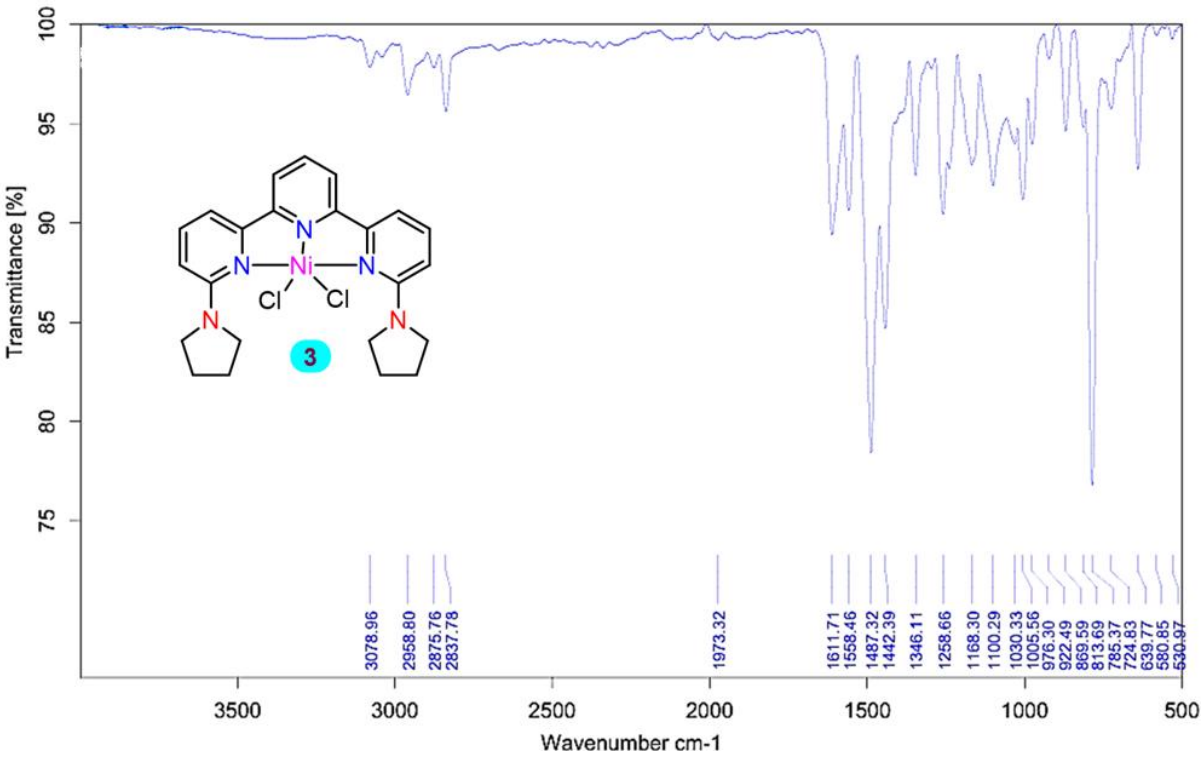

Figure S19. FTIR Spectrum of complex **3**.

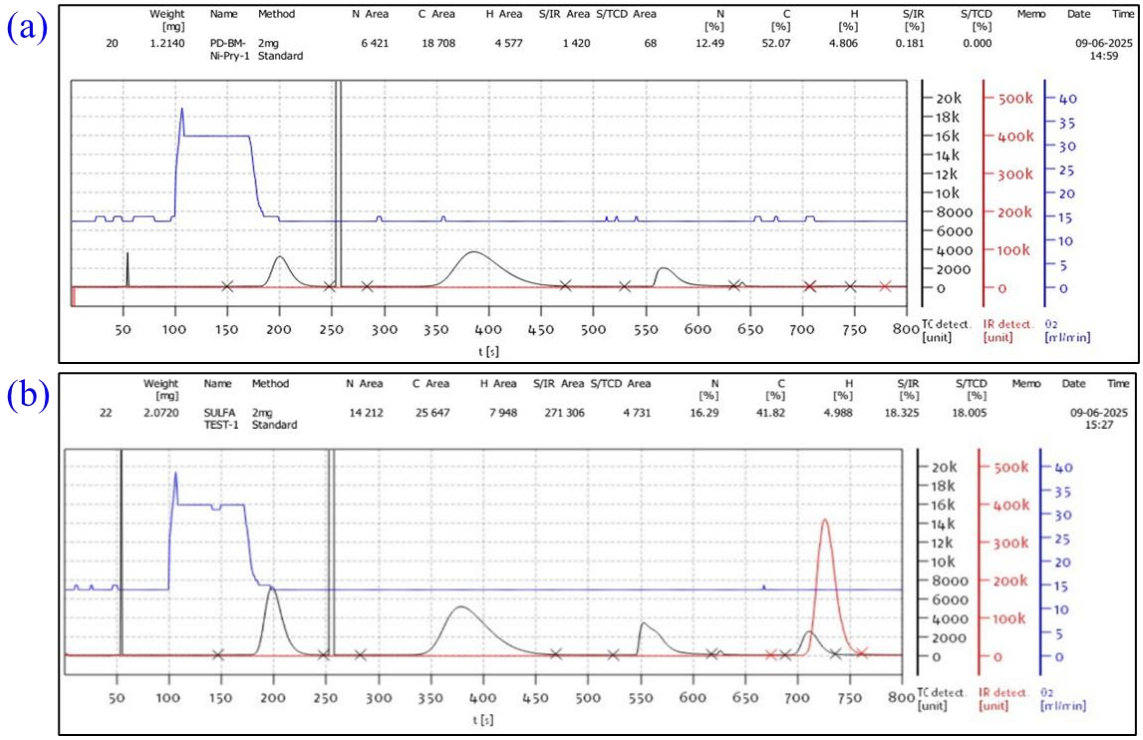

Figure S20. CHNS analysis of complex **3,** (a) and Sulphanilamide standard test (b).

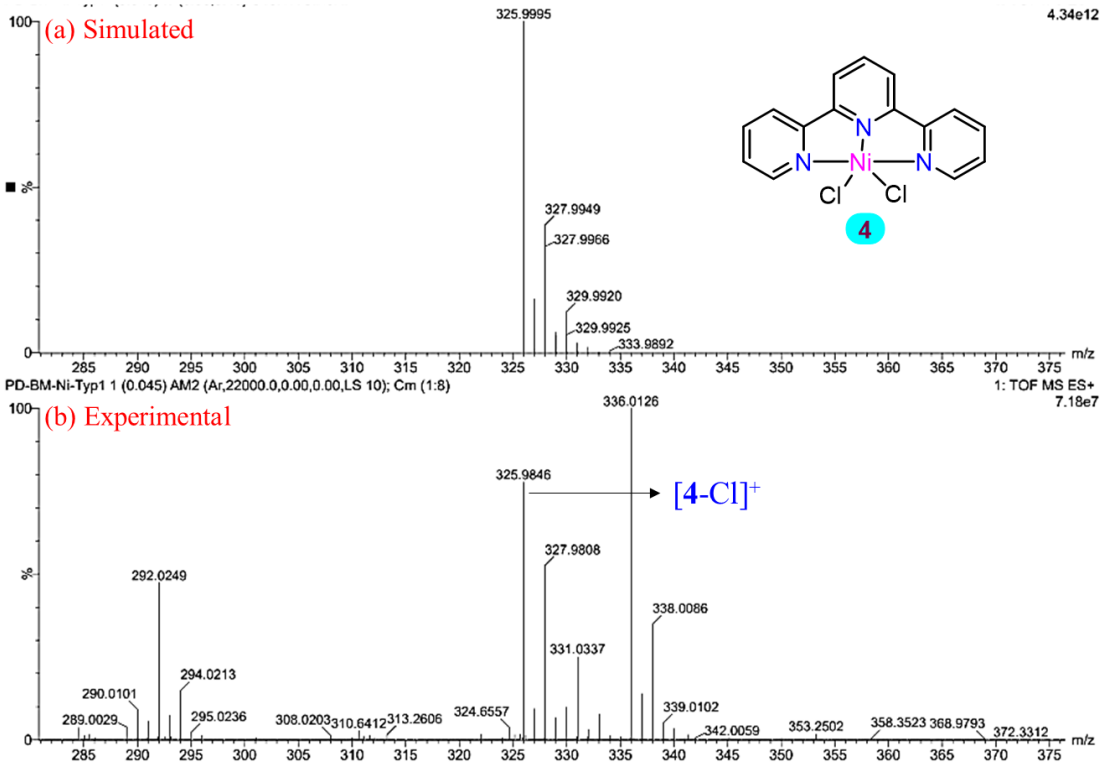

Figure S21. Isotopic mass distribution analysis of complex **4**. Simulated (a) and Experimental. (b).

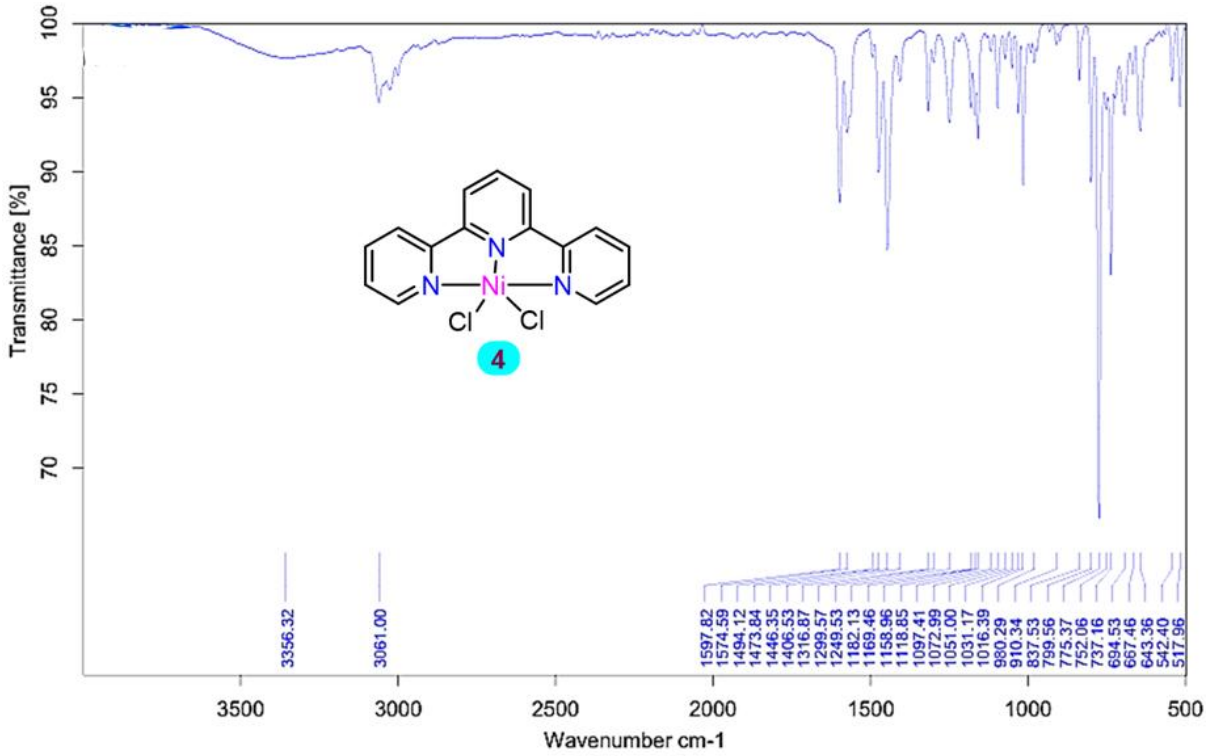

Figure S22. FTIR Spectrum of complex **4**.

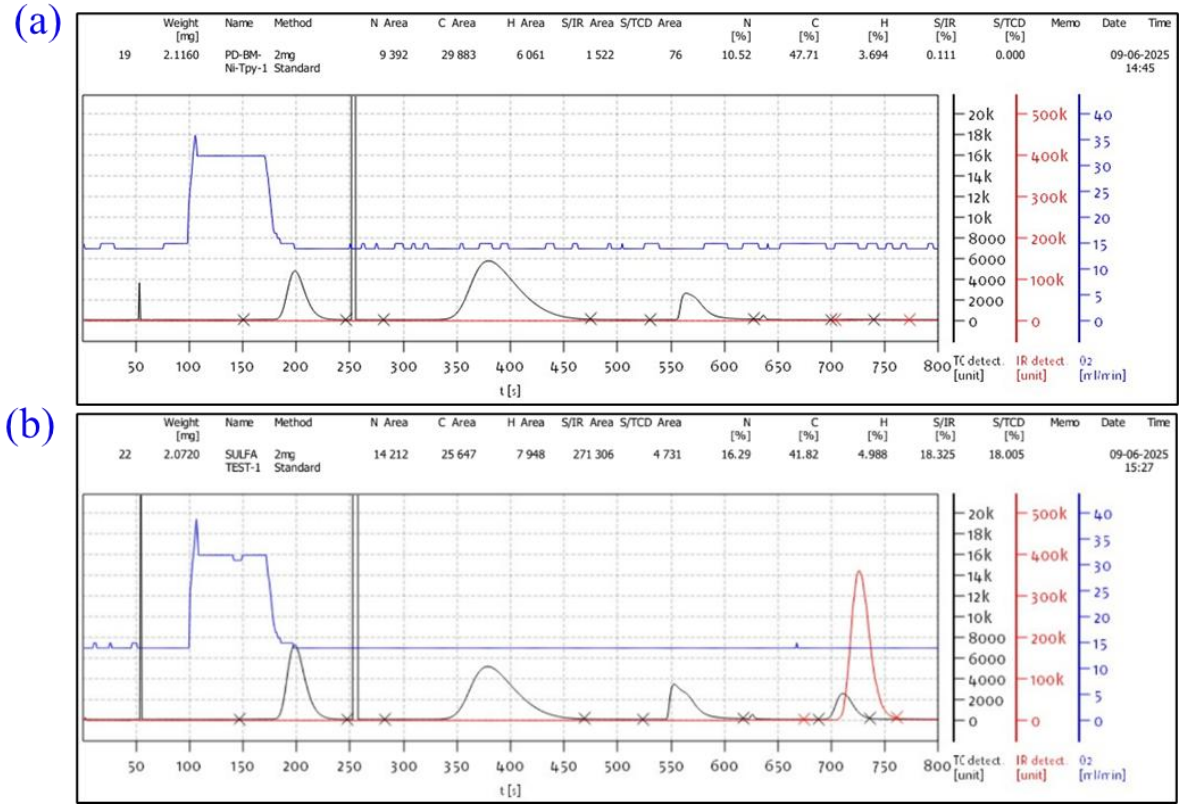

Figure S23. CHNS analysis of complex **4,** (a) and Sulphanilamide standard test (b).

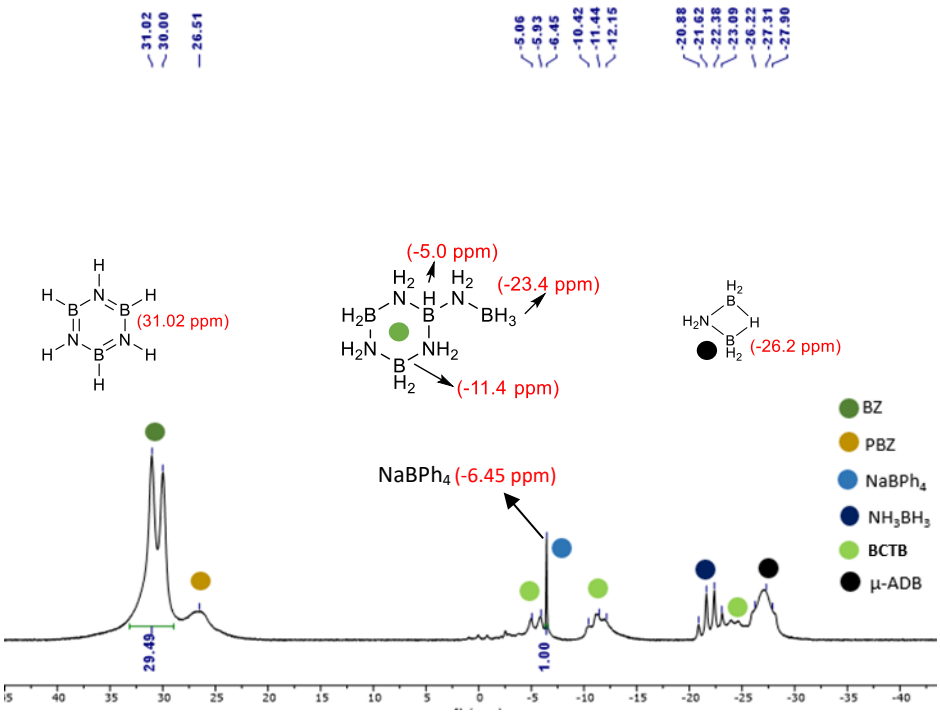

Figure S24. ^{11}B NMR analysis of AB dehydrogenation (Table S1, entry 1)

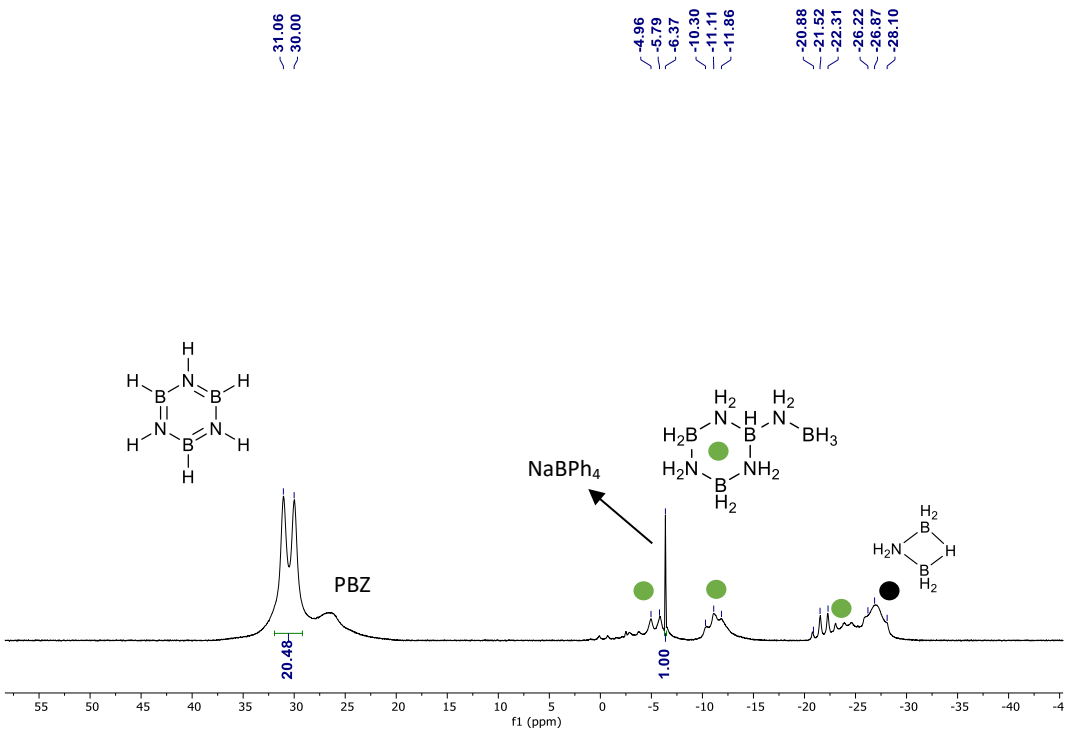

Figure S25. ^{11}B NMR analysis of AB dehydrogenation (Table S1, entry 2)

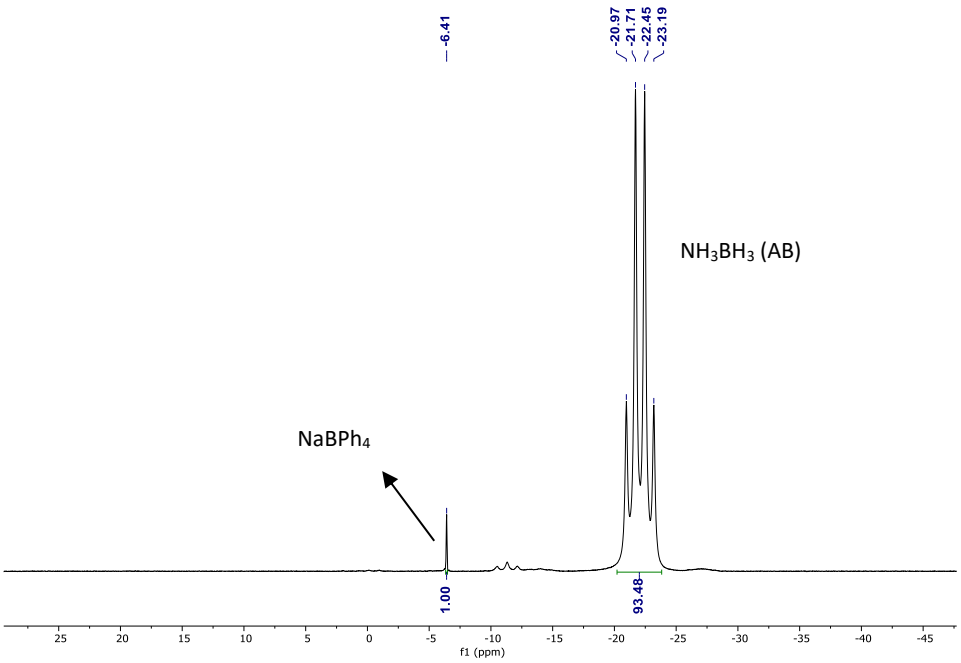

Figure S26. ^{11}B NMR analysis of AB dehydrogenation (Table S1, entry 3)

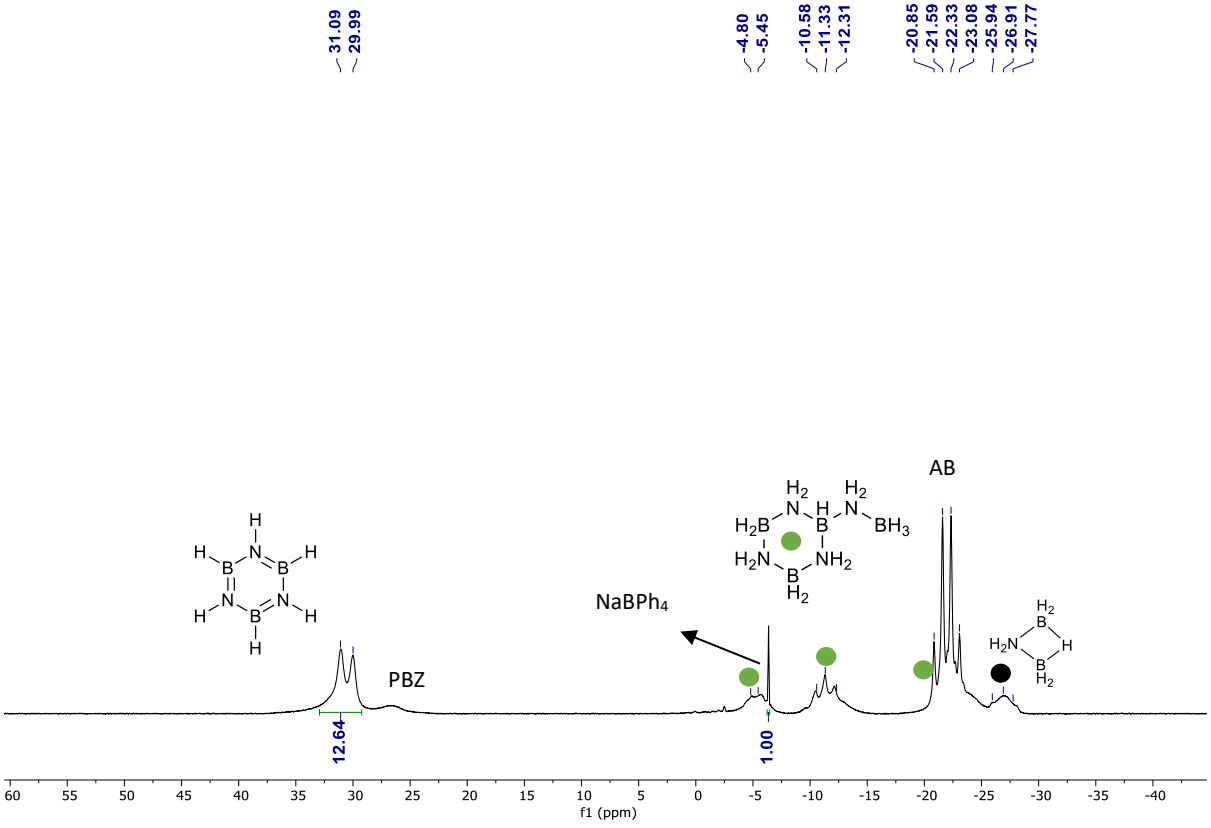

Figure S27. ^{11}B NMR analysis of AB dehydrogenation (Table S1, entry 4)

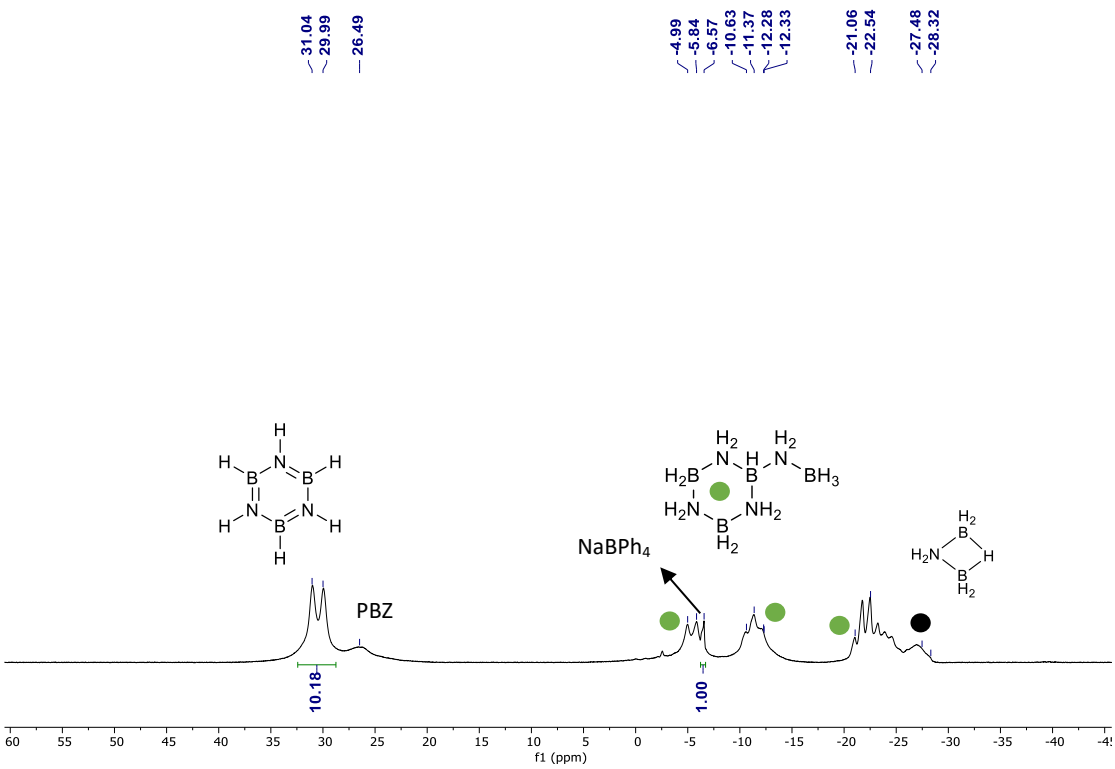

Figure S28. ^{11}B NMR analysis of AB dehydrogenation (Table S1, entry 5)

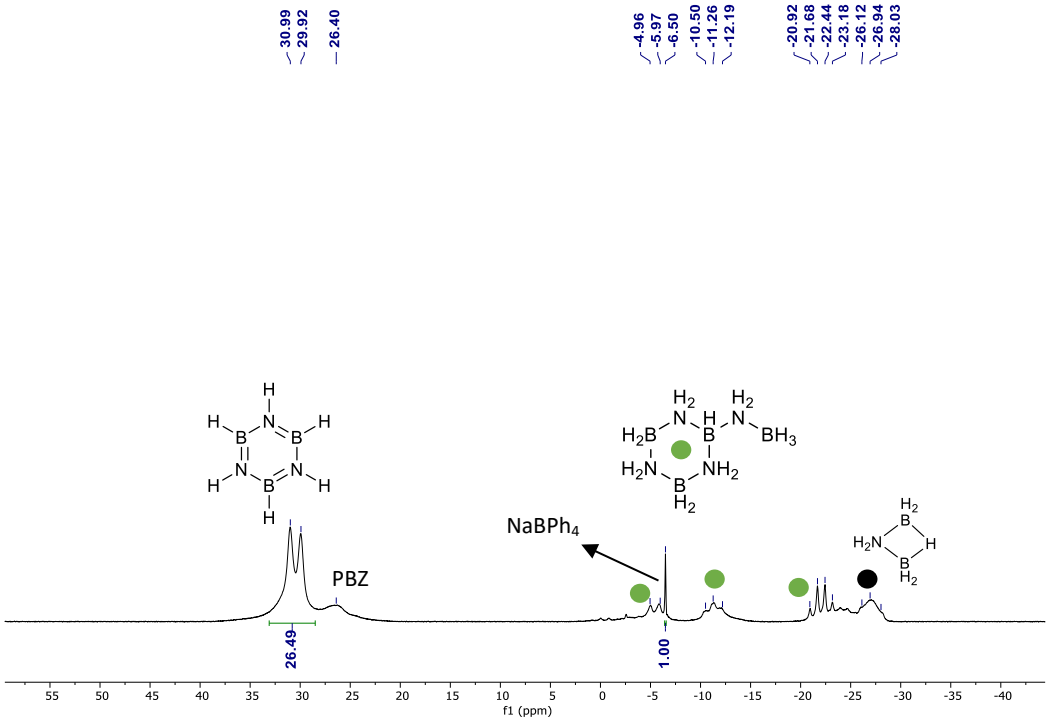

Figure S29. ^{11}B NMR analysis of AB dehydrogenation (Table S1, entry 6)

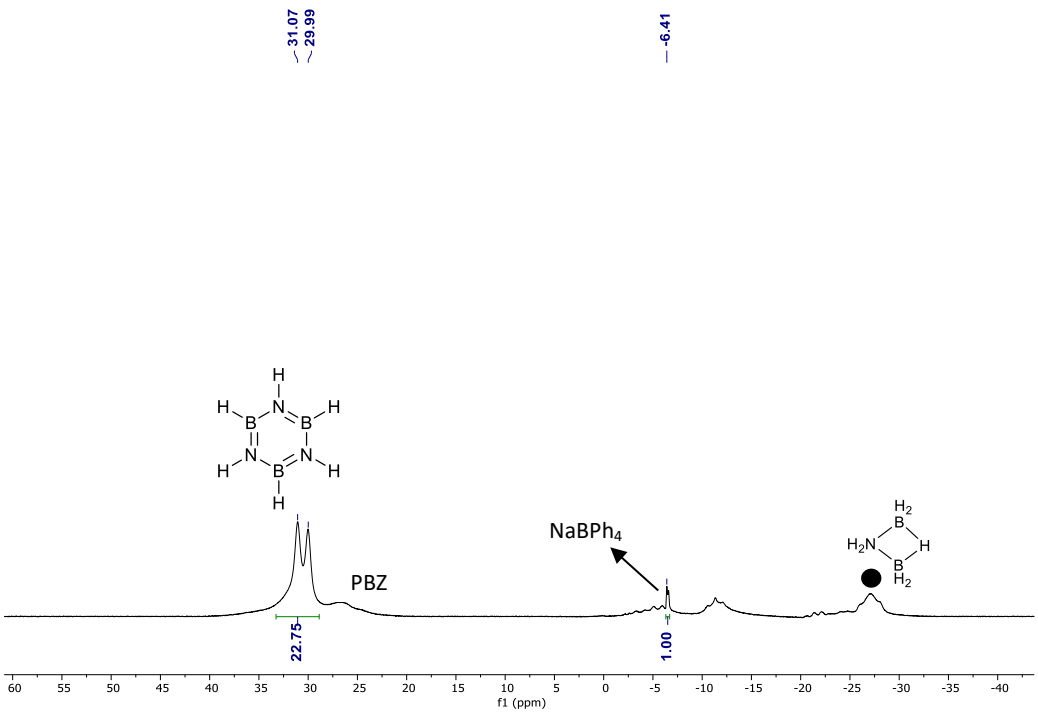

Figure S30. ^{11}B NMR analysis of AB dehydrogenation (Table S1, entry 7)

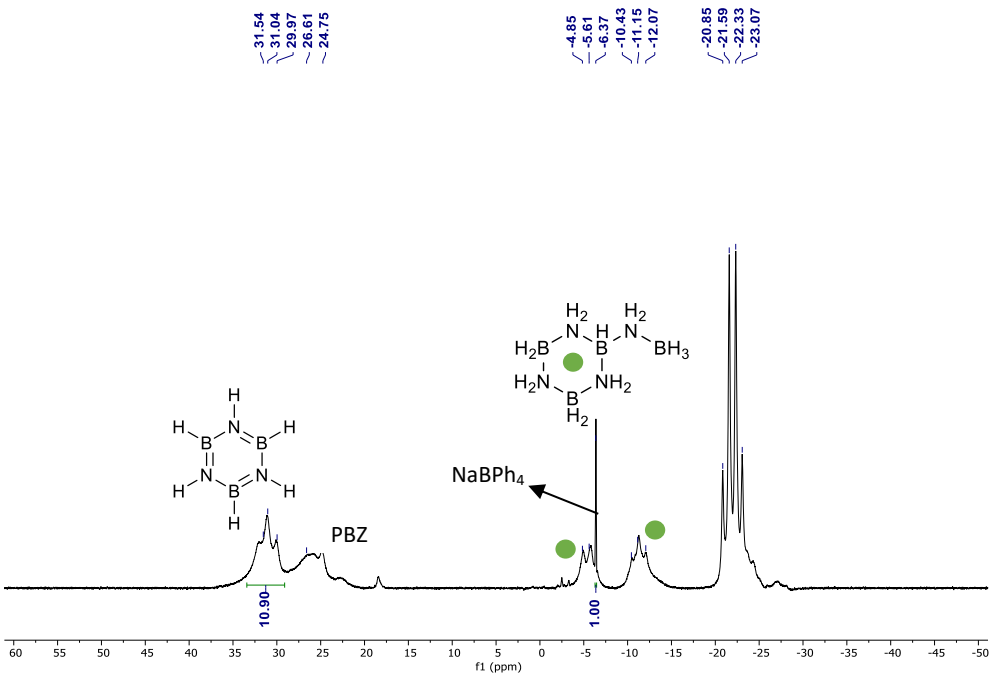

Figure S31. ^{11}B NMR analysis of AB dehydrogenation (Table S1, entry 8)

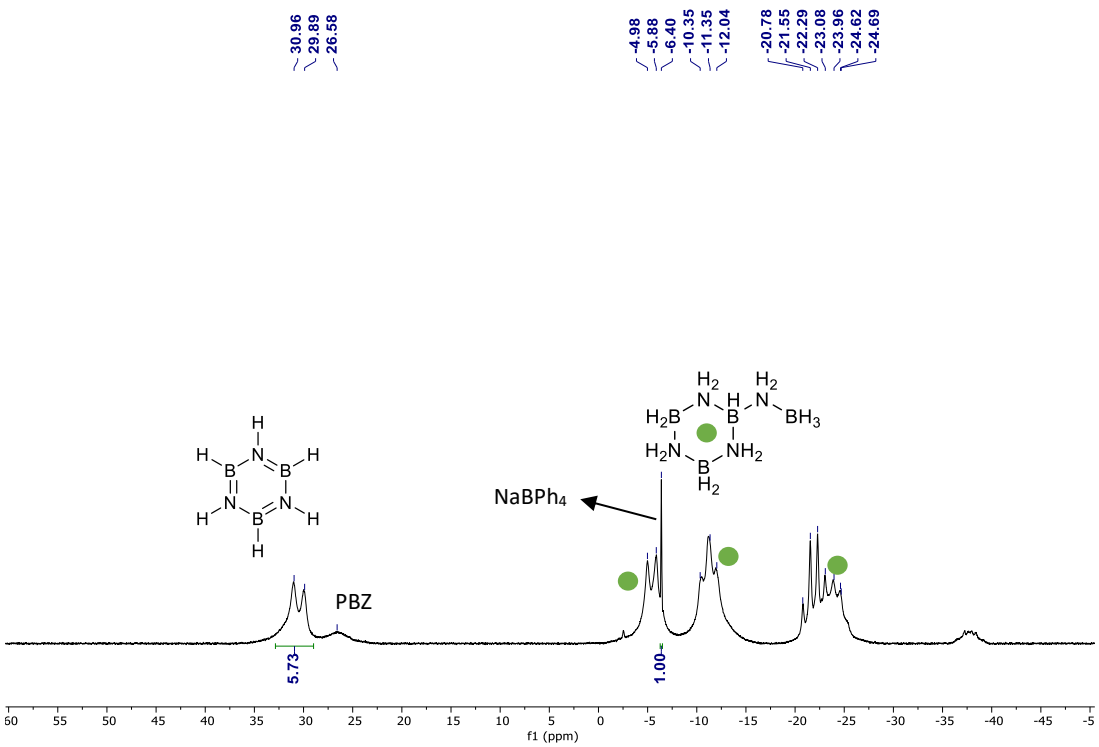

Figure S32. ^{11}B NMR analysis of AB dehydrogenation (Table S1, entry 9)

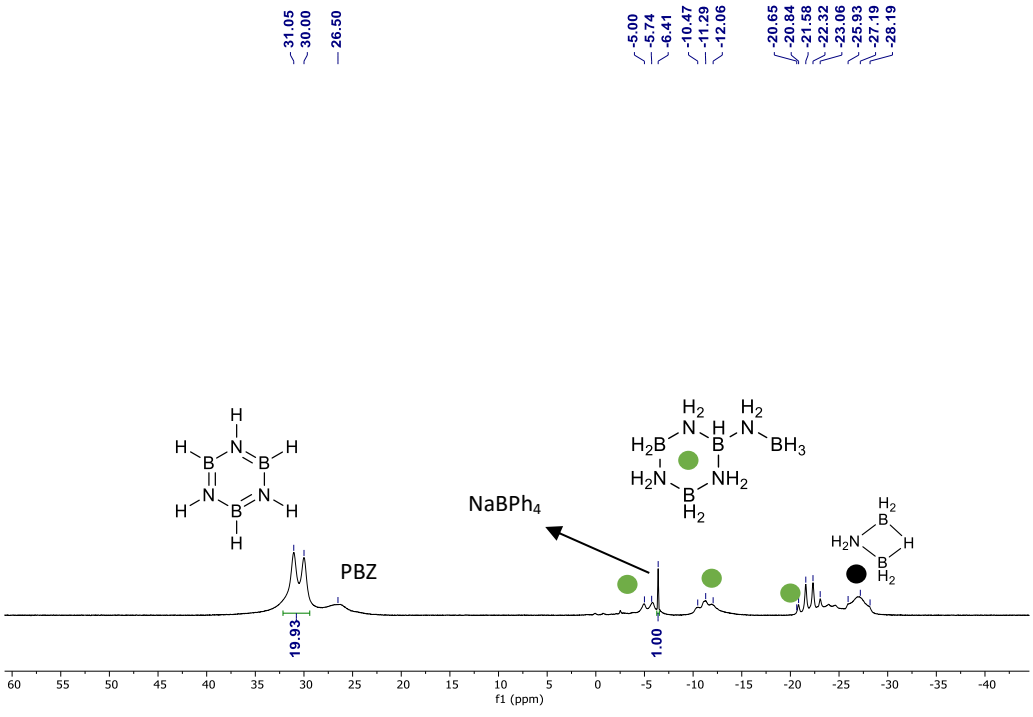

Figure S33. ^{11}B NMR analysis of AB dehydrogenation (Table S1, entry 10)

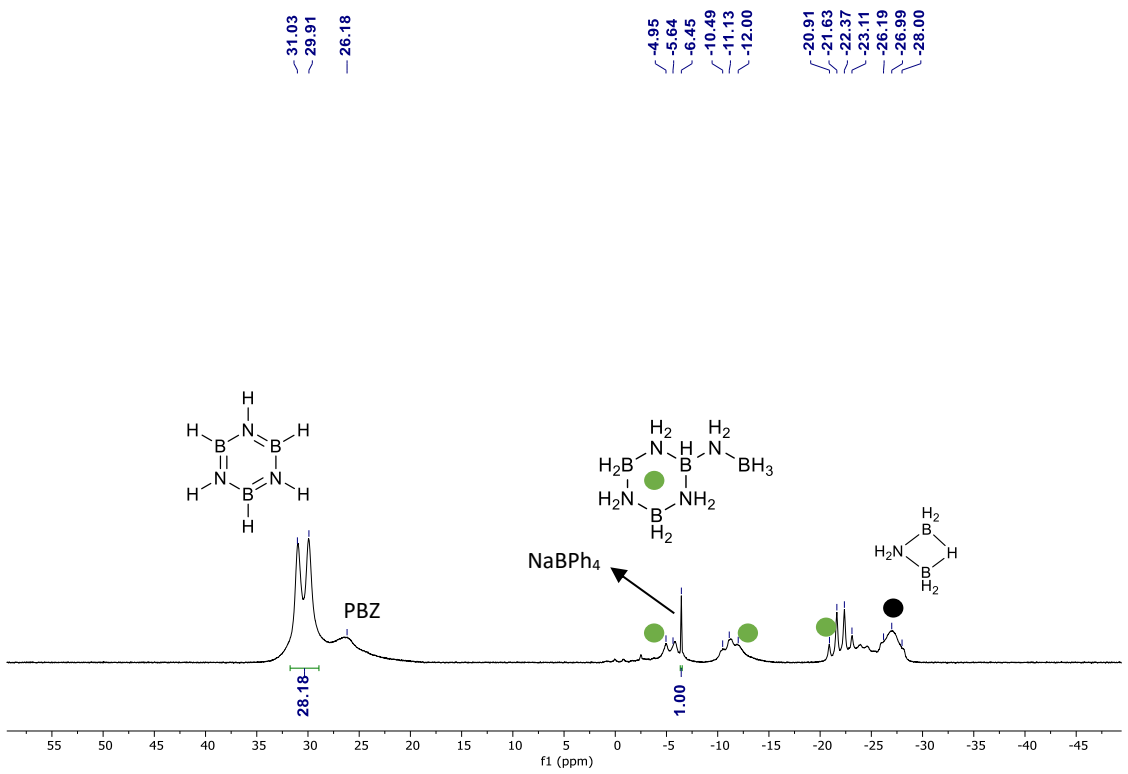

Figure S34. ^{11}B NMR analysis of AB dehydrogenation (Table S1, entry 11)

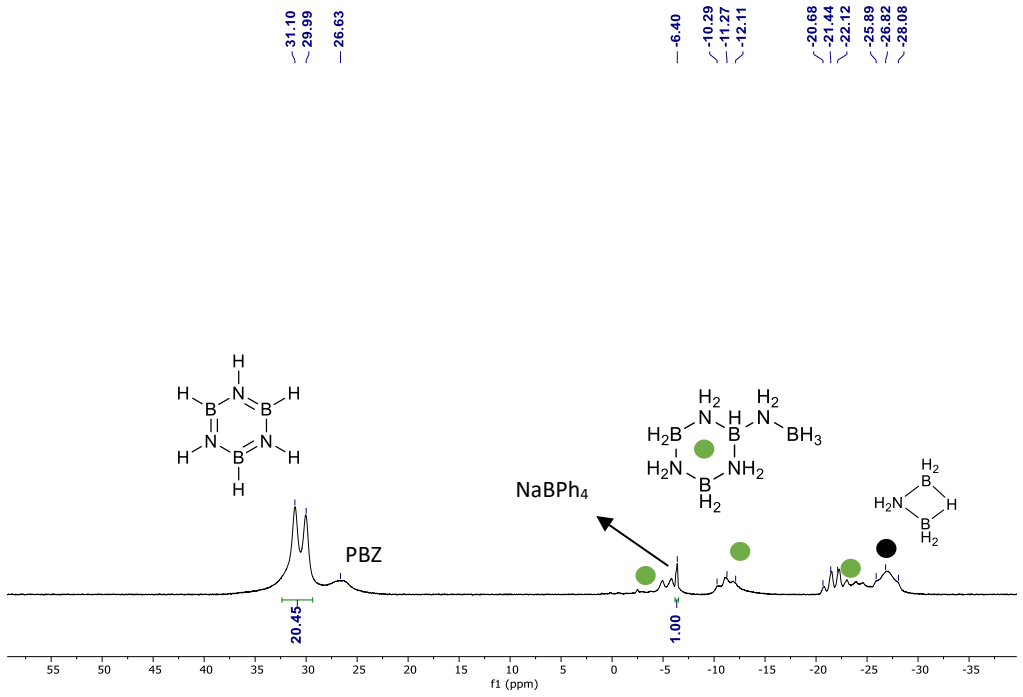

Figure S35. ^{11}B NMR analysis of AB dehydrogenation (Table S1, entry 12)

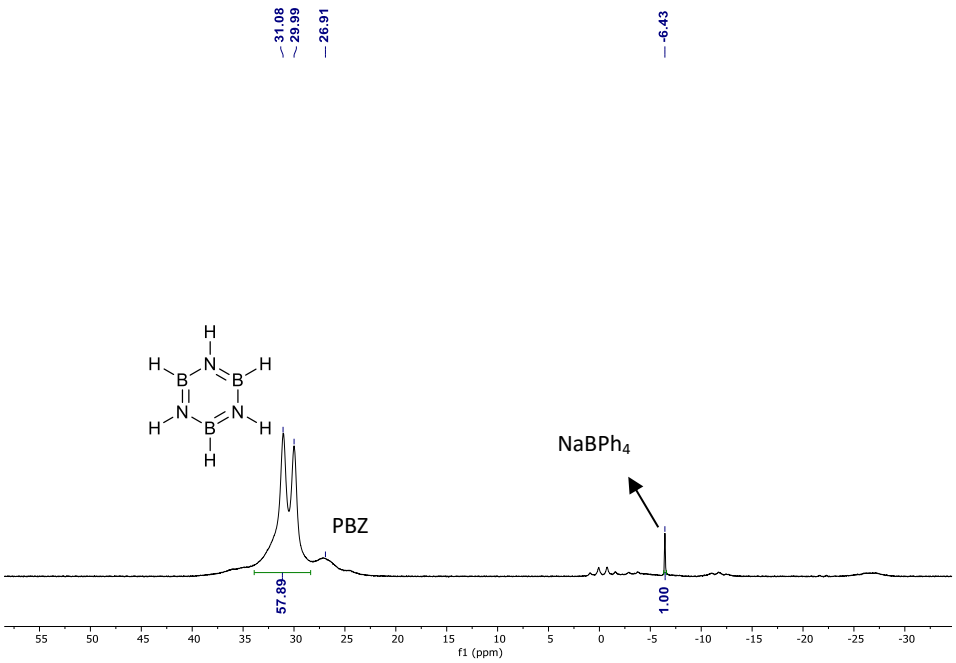

Figure S36. ^{11}B NMR analysis of AB dehydrogenation (Table S1, entry 13)

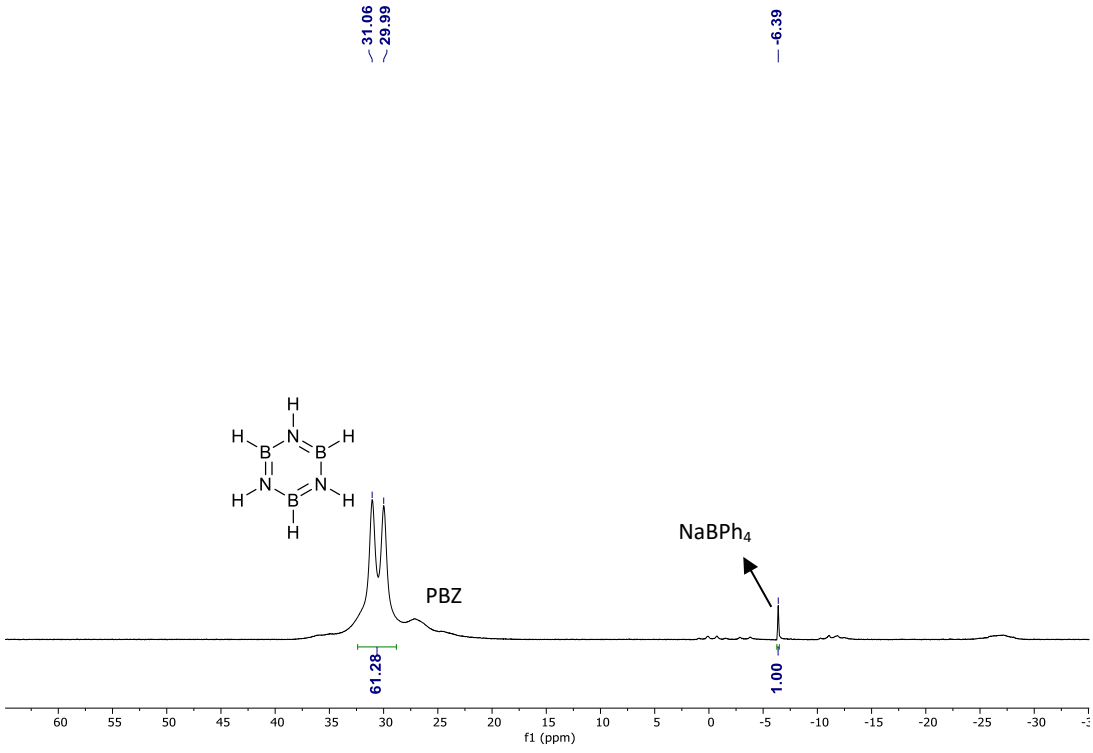

Figure S37. ^{11}B NMR analysis of AB dehydrogenation (Table S1, entry 14)

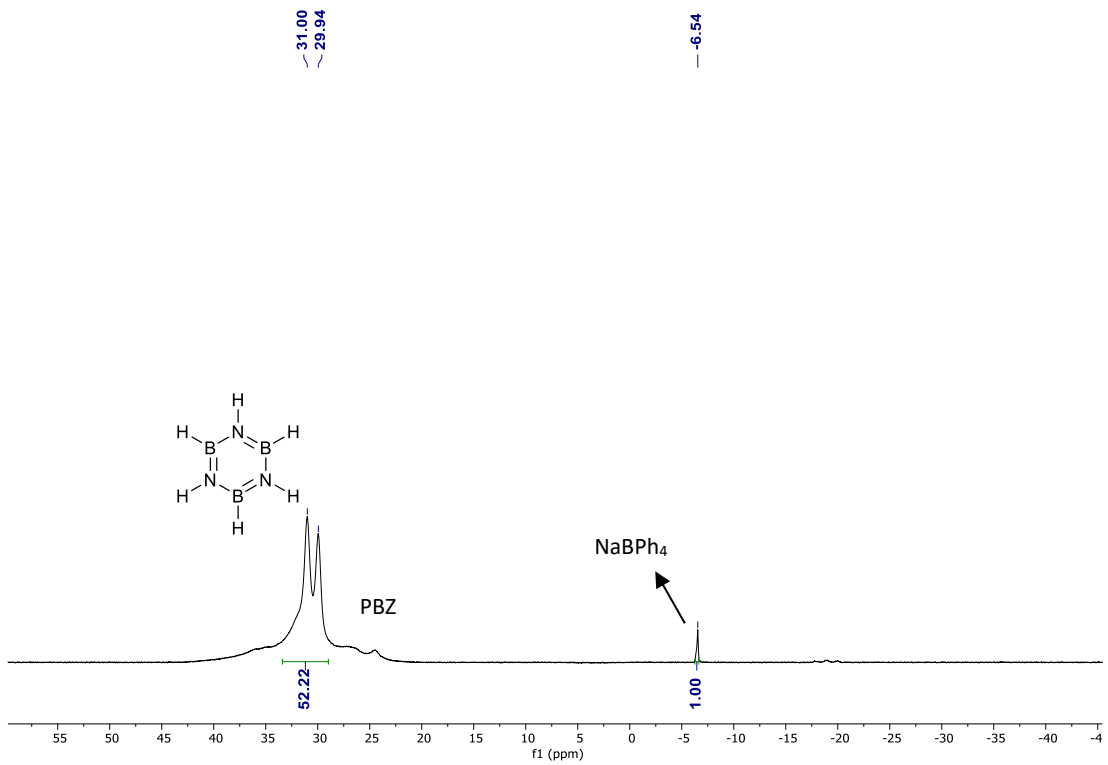

Figure S38. ^{11}B NMR analysis of AB dehydrogenation (Table S1, entry 15)

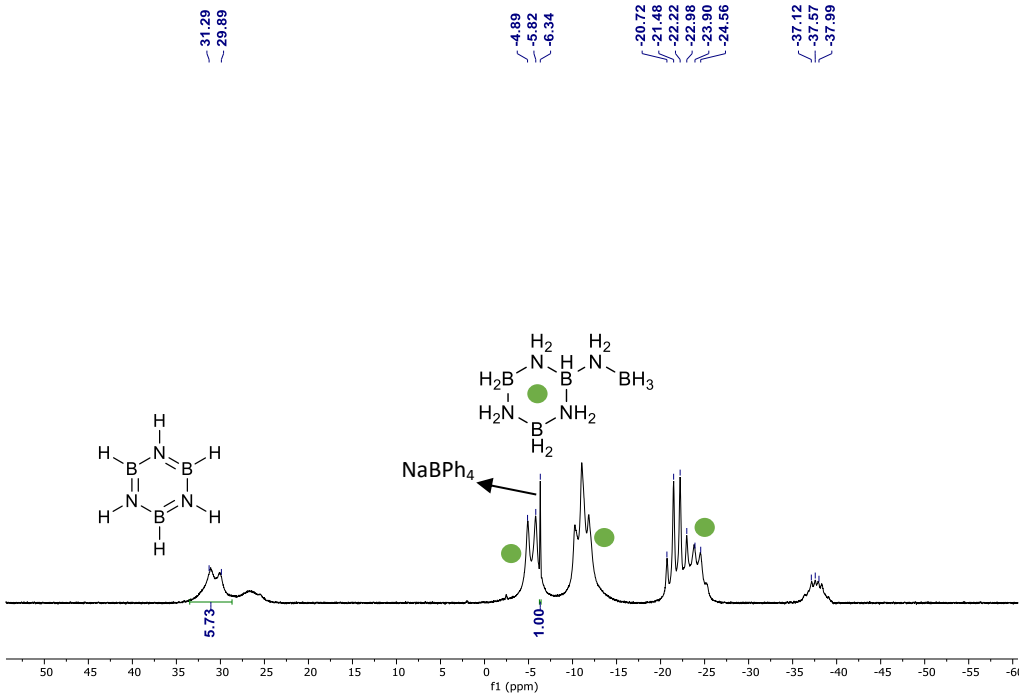

Figure S39. ^{11}B NMR analysis of AB dehydrogenation with PPh_3 (Table S1, entry 16)

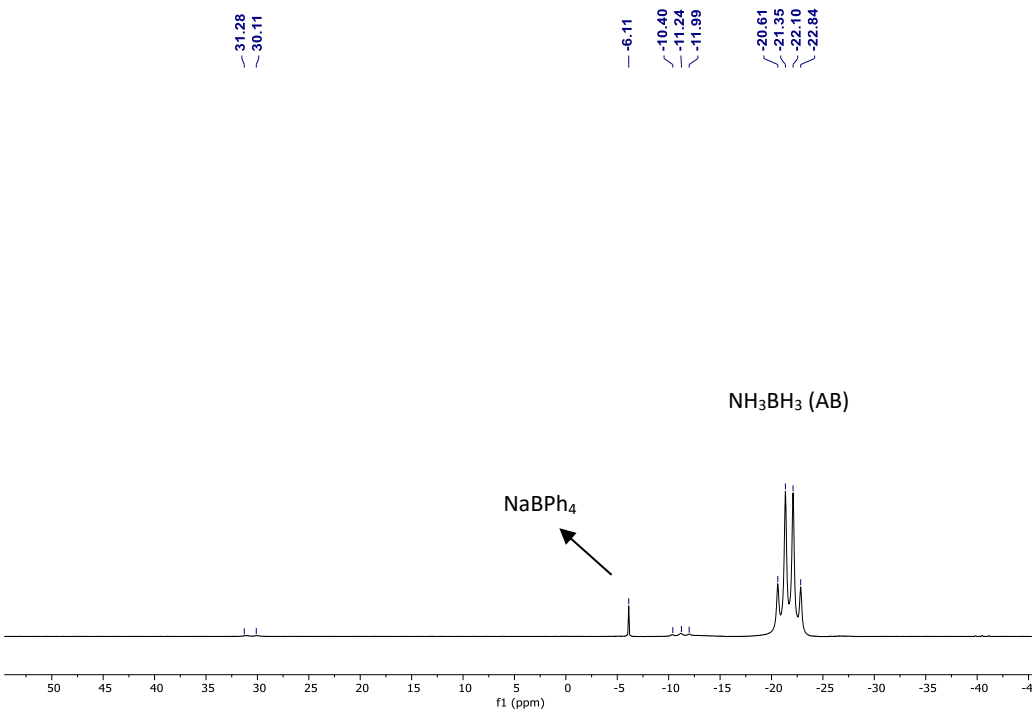

Figure S40. ^{11}B NMR analysis of AB dehydrogenation (Table S1, entry 17)

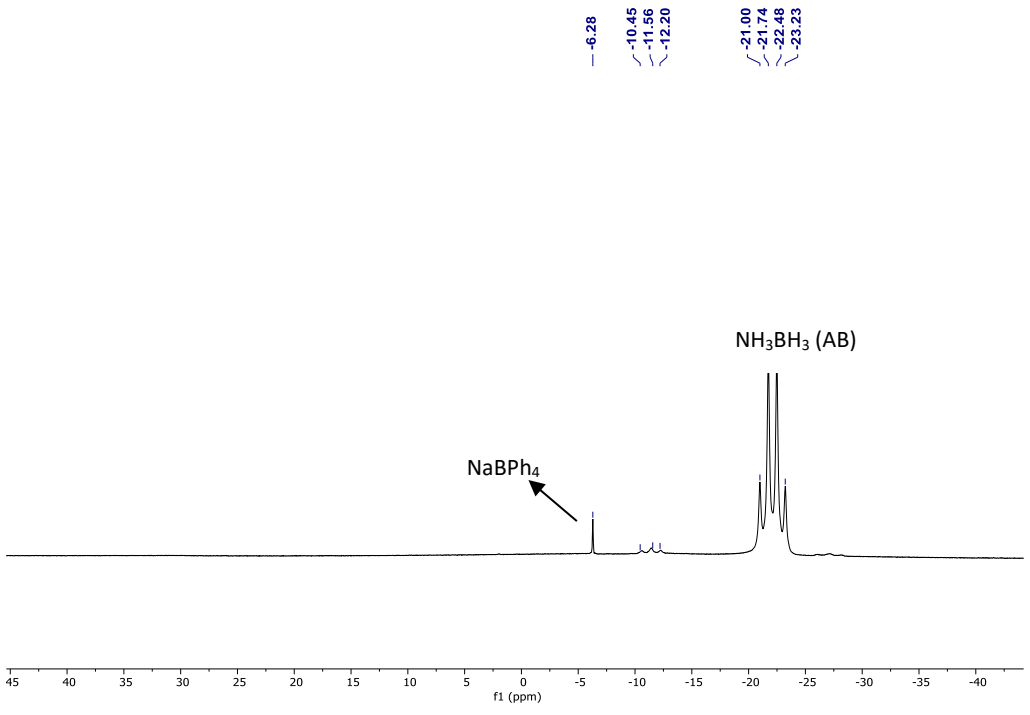

Figure S41. ^{11}B NMR analysis of AB dehydrogenation (Table S1, entry 18)

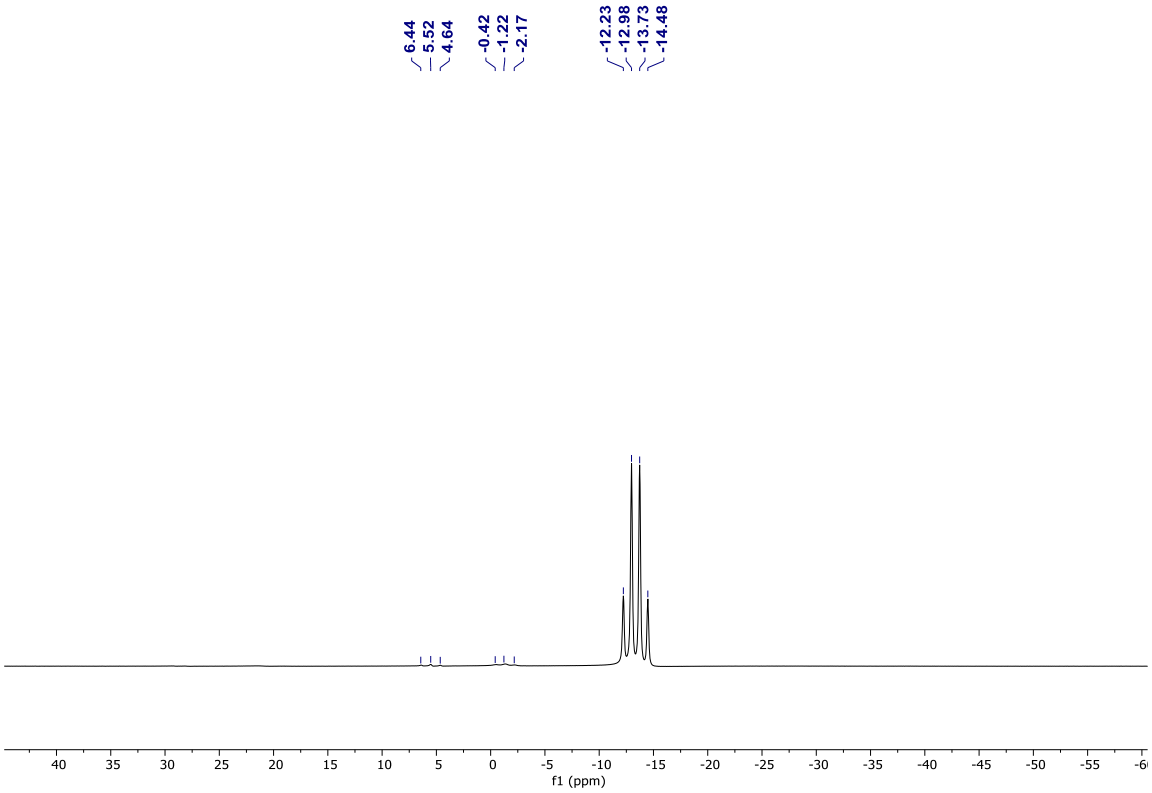

Figure S42. ^{11}B NMR analysis of Me_2NHBH_3 dehydrogenation (Table S1, entry 19)

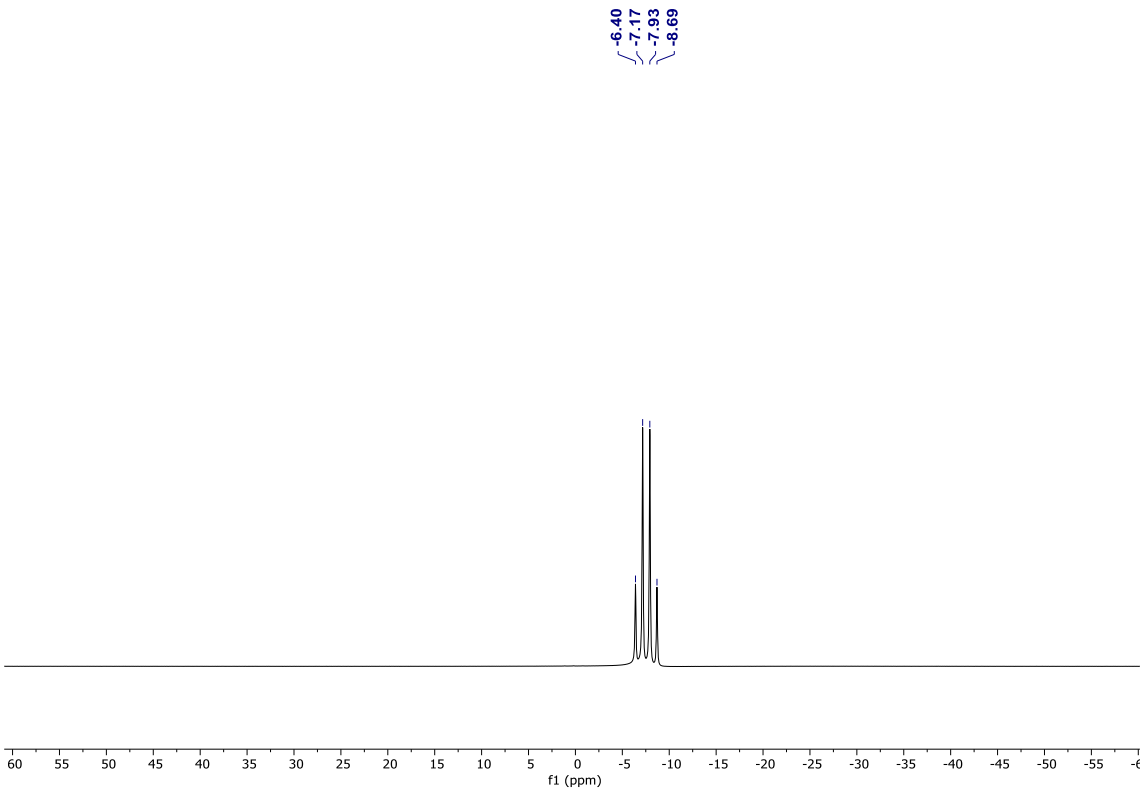

Figure S43. ^{11}B NMR analysis of Me_3NBH_3 dehydrogenation (Table S1, entry 20)

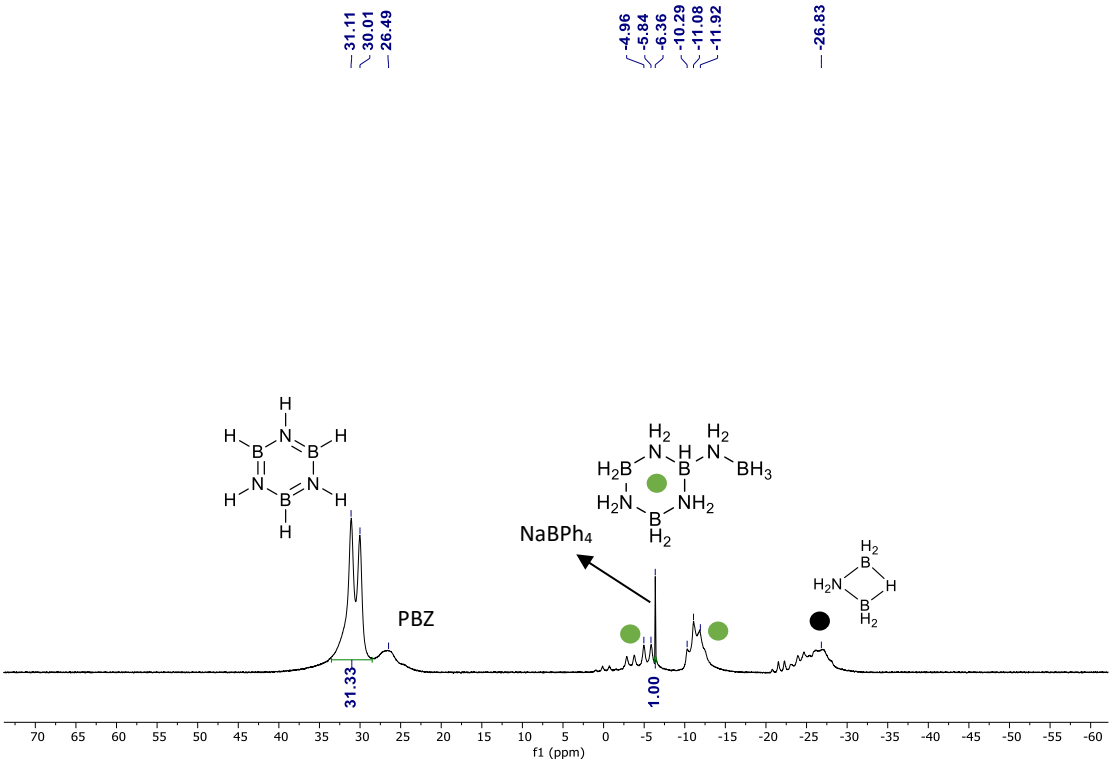

Figure S44. ^{11}B NMR analysis of AB dehydrogenation (Table S2, entry 1). Internal standard (0.01 mmol)

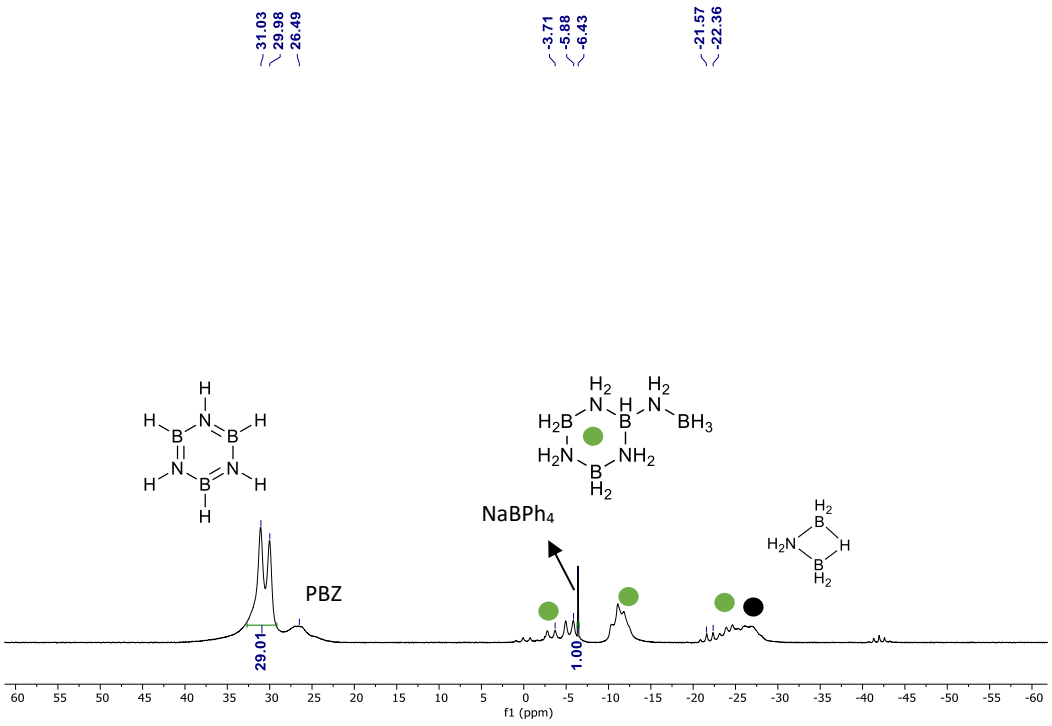

Figure S45. ^{11}B NMR analysis of AB dehydrogenation (Table S2, entry 2). Internal standard (0.01 mmol)

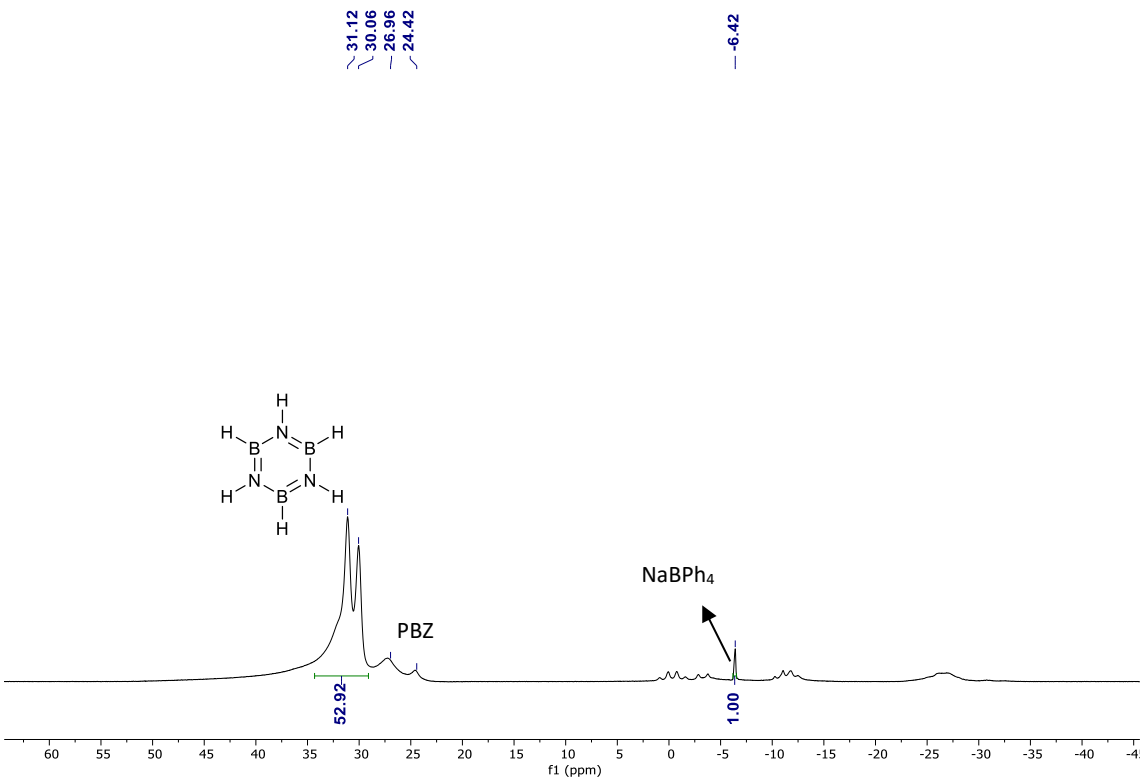

Figure S46. ^{11}B NMR analysis of AB dehydrogenation (Table S2, entry 3). Internal standard (0.05 mmol)

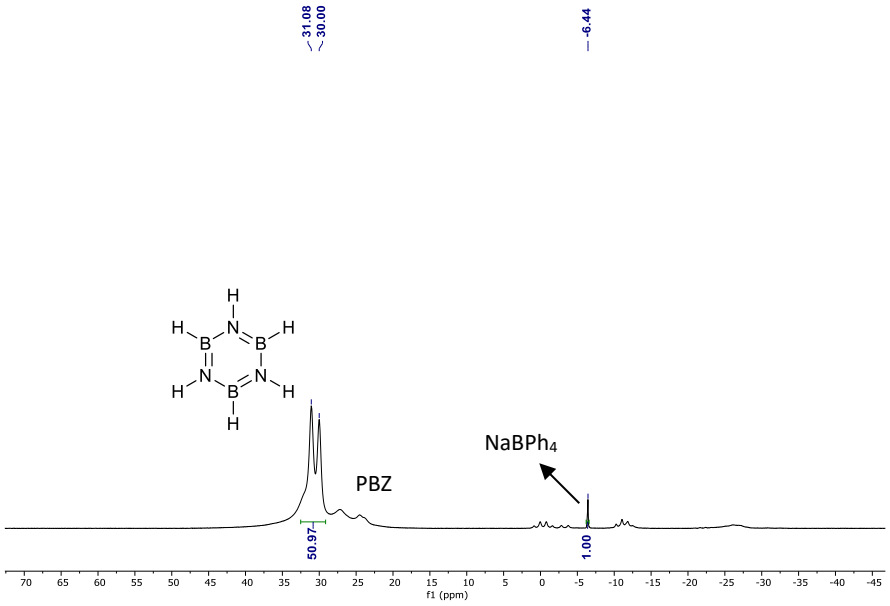

Figure S47. ^{11}B NMR analysis of AB dehydrogenation (Table S2, entry 4). Internal standard (0.1 mmol)

9. X-Ray Crystallographic data

9.1. Crystal data of complex 2

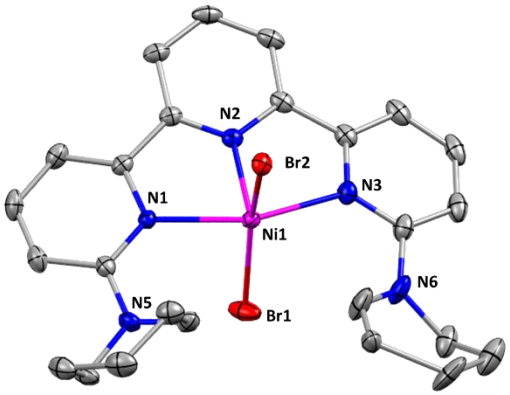

Figure S48. Molecular structure of complex **2**

Table S3. Crystal data and structure refinement for complex **2**

Name	Complex **2**
CCDC Number	**2496603**
Empirical formula	$C_{25}H_{29}Br_2N_5Ni$
Formula weight	616.04
Temperature/K	100.15
Crystal system	monoclinic
Space group	$P2_1/c$
a/Å	9.04470(10)
b/Å	28.1677(2)
c/Å	9.31320(10)
α/°	90
β/°	90.3480(10)
γ/°	90
Volume/Å^3	2372.67(4)
Z	4
ρ_{calc}g/cm^3	1.725
μ/mm^{-1}	5.309
F(000)	1240.0
Crystal size/mm^3	0.4 × 0.3 × 0.2
Radiation	CuKα (λ = 1.54184)
2Θ range for data collection/°	6.276 to 150.704
Index ranges	$-11 \le h \le 11$, $-34 \le k \le 34$, $-11 \le l \le 10$
Reflections collected	82923
Independent reflections	4804 [R_{int} = 0.0426, R_{sigma} = 0.0134]
Data/restraints/parameters	4804/382/363
Goodness-of-fit on F^2	1.060
Final R indexes [I>=2σ (I)]	R_1 = 0.0247, wR_2 = 0.0670
Final R indexes [all data]	R_1 = 0.0253, wR_2 = 0.0674
Largest diff. peak/hole / e Å^{-3}	0.66/-0.54

9.2. Crystal data of complex 3

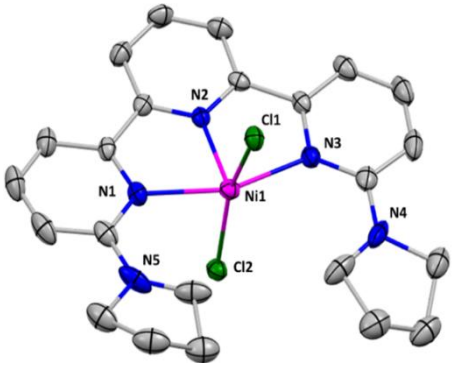

Figure S49. Molecular structure of complex **3**

Table S4. Crystal data and structure refinement for complex **3**

Name	Complex **3**
CCDC Number	**2496604**
Empirical formula	$C_{11.5}H_{12.5}ClN_{2.5}Ni_{0.5}$
Formula weight	250.54
Temperature/K	100.15
Crystal system	monoclinic
Space group	C2/c
a/Å	11.16250(10)
b/Å	12.33170(10)
c/Å	15.6518(2)
α/°	90
β/°	101.7910(10)
γ/°	90
Volume/Å^3	2109.05(4)
Z	8
ρ_{calc}g/cm^3	1.578
μ/mm^{-1}	3.829
F(000)	1040.0
Crystal size/mm^3	0.5 × 0.3 × 0.2
Radiation	CuKα (λ = 1.54184)
2Θ range for data collection/°	10.818 to 154.176
Index ranges	$-13 \leq h \leq 13$, $-15 \leq k \leq 15$, $-19 \leq l \leq 19$
Reflections collected	25445
Independent reflections	2199 [R_{int} = 0.0349, R_{sigma} = 0.0160]
Data/restraints/parameters	2199/234/150
Goodness-of-fit on F^2	1.083
Final R indexes [I>=2σ (I)]	R_1 = 0.0433, wR_2 = 0.1077
Final R indexes [all data]	R_1 = 0.0465, wR_2 = 0.1096
Largest diff. peak/hole / e Å^{-3}	1.29/-0.54

9.3. Crystal data of complex 4

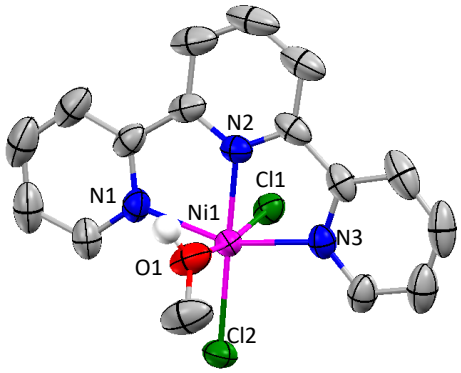

Figure S50. Molecular structure of complex **4**.MeOH

Table S5. Crystal data and structure refinement for complex **4**.MeOH

Name	Complex **4**.MeOH
CCDC Number	**2496605**
Empirical formula	$C_{16}H_{15}Cl_2N_3NiO$
Formula weight	394.92
Temperature/K	300.15
Crystal system	monoclinic
Space group	$P2_1/c$
a/Å	9.31157(5)
b/Å	6.89229(4)
c/Å	25.41149(18)
α/°	90
β/°	92.3034(6)
γ/°	90
Volume/Å^3	1629.543(18)
Z	4
ρ_{calc}g/cm^3	1.610
μ/mm^{-1}	4.789
F(000)	808.0
Crystal size/mm^3	0.5 × 0.3 × 0.2
Radiation	CuKα (λ = 1.54184)
2Θ range for data collection/°	6.962 to 131.326
Index ranges	$-11 \leq h \leq 10$, $-8 \leq k \leq 8$, $-29 \leq l \leq 30$
Reflections collected	33655
Independent reflections	2800 [R_{int} = 0.0225, R_{sigma} = 0.0095]
Data/restraints/parameters	2800/174/249
Goodness-of-fit on F^2	1.077
Final R indexes [I>=2σ (I)]	R_1 = 0.0232, wR_2 = 0.0608
Final R indexes [all data]	R_1 = 0.0249, wR_2 = 0.0618
Largest diff. peak/hole / e Å^{-3}	0.22/-0.19

10. Proton coupled and decoupled ^{11}B NMR for borazine

To ensure the borazine structure formation, Table S1, entry 14 was repeated and checked for proton-coupled and proton decoupled ^{11}B NMR.

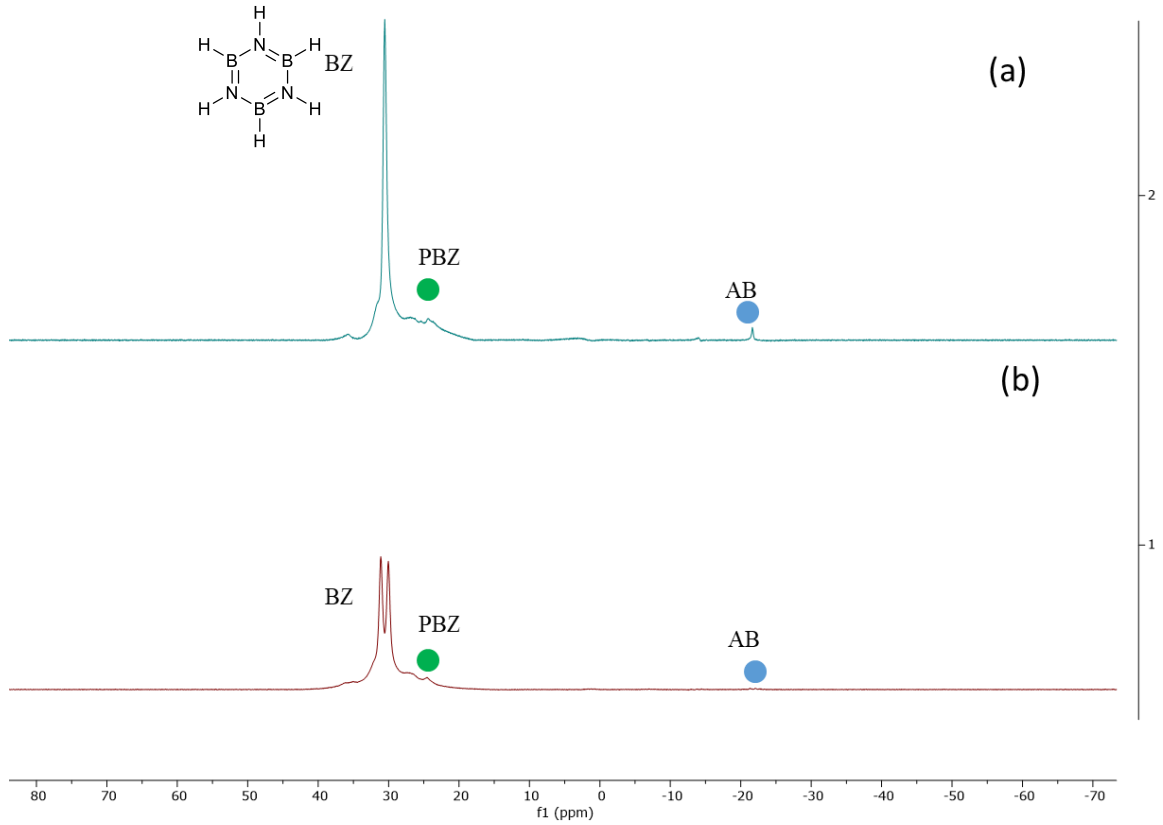

Figure S51. ^{11}B NMR with proton-decoupled(a) and proton-coupled (b) analysis of AB dehydrogenation.

11.References

1 C. D. Mboyi, S. Gaillard, M. D. Mabaye, N. Pannetier and J.-L. Renaud, *Tetrahedron*, 2013, **69**, 4875–4882.

2 P. Jurt, J. J. Gamboa-Carballo, C. Schweinzer, D. Himmelbauer, D. Thöny, T. L. Gianetti, M. Trincado and H. Grützmacher, *Dalt. Trans.*, 2024, **53**, 14212–14218.

3 X. Yang, L. Zhao, T. Fox, Z. X. Wang and H. Berke, *Angew. Chem. Int. Ed.*, 2010, **49**, 2058–2062.

4 A. M. W. Cargill Thompson, *Coord. Chem. Rev.*, 1997, **160**, 1–52.

5 V. V. Zamalyutin, V. A. Bezdenezhnykh, A. I. Nichugovskiy and V. R. Flid, *Russ. J.*

Org. Chem., 2018, **54**, 419–425.

6 A. Mohanty, S. R. Rout, R. Dandela and P. Daw, *Chem. Commun.*, 2024, **60**, 416–419.

7 A. Mohanty, A. Sinha, G. Kenguva, R. Dandela and P. Daw, *ChemCatChem*, 2025, **17**, 2–9.

8 S. T. Sahoo, A. Mohanty, R. Sharma and P. Daw, *Dalt. Trans.*, 2023, **52**, 15343–15347.

9 S. Bhunya, P. M. Zimmerman and A. Paul, *ACS Catal.*, 2015, **5**, 3478–3493.

10 S. Todisco, L. Luconi, G. Giambastiani, A. Rossin, M. Peruzzini, I. E. Golub, O. A. Filippov, N. V. Belkova and E. S. Shubina, *Inorg. Chem.*, 2017, **56**, 4296–4307.

11 C. A. Castilla-Martinez, P. Gaveau, M. Semsarilar, B. Alonso and U. B. Demirci, *Chem. – An Asian J.*, DOI:10.1002/asia.202500140.